

# **Operational Software Developments**



**On the Accuracy of ERS-1 Orbit Predictions**

presented at  
8th International Workshop on Laser Ranging Instrumentation  
Annapolis, MD USA  
May 18-22, 1992  
by

R. König, H. Li, F.-H. Massmann, J.C. Raimondo, C. Rajasenan, Ch. Reigber  
Deutsches Geodätisches Forschungsinstitut, Abt.I (DGFI) and  
German Processing and Archiving Facility (D-PAF)  
Münchner Str. 20  
D-8031 Oberpfaffenhofen  
Germany

**Summary**

Since the launch of ERS-1 (first European Remote Sensing Satellite) the D-PAF (German Processing and Archiving Facility) provides regularly orbit predictions for the worldwide SLR (Satellite Laser Ranging) tracking network. The weekly distributed orbital elements are so-called tuned IRVs and tuned SAO-elements. The tuning procedure, designed to improve the accuracy of the recovery of the orbit at the stations, is discussed based on numerical results. This shows that tuning of elements is essential for ERS-1 with the currently applied tracking procedures.

The orbital elements are updated by daily distributed time bias functions. The generation of the time bias function is explained. Problems and numerical results are presented. The time bias function increases the prediction accuracy considerably.

Finally the quality assessment of ERS-1 orbit predictions is described. The accuracy is compiled for about 250 days since launch. The average accuracy lies in the range of 50-100 ms and has considerably improved.

## 1. Background and Introduction

Since the very first days when ERS-1 began his mission in space, the D-PAF is sending orbit predictions to the SLR community. The orbit predictions are produced in form of the well established IRVs and SAO-elements. The procedure is given in chapter 2. Though these orbital elements are very compressed forms of complicated orbit trajectories, they optimally represent the orbit. The trick to achieve this is called *tuning* of elements. In chapter 3 the problem is illuminated from the numerical point of view.

Very soon after launch it became clear that the ERS-1 trajectory is extremely affected by solar and geomagnetic activities. The orbit predictions lost accuracy mainly in along-track direction. The D-PAF therefore introduced the time bias function which is generated and disseminated daily. Meanwhile the time bias function has become an accepted tool in the SLR community. Some features of the time bias function and related topics are explained in chapter 4.

The extremely high solar activity in the first months of the mission brought extraordinary events such as a geomagnetic storm of nearly singular type. Though SLR tracking was almost lost for two days, the D-PAF orbit prediction system (and the SLR community in turn) gained at the end. The software system got more backup solutions and the quality checks were largely extended. Chapter 5 tells more about quality assessment and quality checks.

Finally the orbit prediction system has developed to a reliable system in SLR tracking. This becomes obvious from the course of the average accuracy of the orbit predictions shown in the more detailed analysis in chapter 5.

## 2. Generation of Orbit Predictions

In a first step the orbital parameters are estimated by differential orbit correction with the DOGS-OC (DGFI Orbit and Geodetic parameter estimation System - Orbit Computation) software. Laser ranges are mainly used as observations for the least squares procedure and in few cases also RA FD data (Radar Altimeter Fast Delivery) ( *Massmann, F.-H. et.al., 1992* ). The use of PRARE data (Precise Range And Range rate Equipment) was also planned prior to launch.

Orbit perturbation models used are state of the art ones. The gravitational forces are mainly represented by the GRIM4-S2 gravity field model ( *Schwintzer, P. et.al., 1992* ). The major non-gravitational perturbations of the low altitude orbit stem from surface forces. DOGS-OC adopts a macro model of the surface of ERS-1 for albedo, direct solar radiation and drag. Earth's high atmosphere is represented by the CIRA'86 model where solar and geomagnetic activity is needed as input.

In a second step the orbit is integrated forward by the DOGS-OC software with the parameters derived before. Adopted are the same perturbation models but now solar and geomagnetic activity are predicted for the respective time period. And this indeed is the major error source that degrades the accuracy of ERS-1 orbit predictions. Also the ERPs (Earth rotation parameters) are predicted for the time period of the forward integration. The accuracy of ERP predictions is quite good for the lifetime of ERS-1 orbit predictions, the effect can therefore be neglected.

In the third step DOGS-PD (PD for Predictions) compresses the orbit to dedicated forms and formats of orbital elements which can easily be disseminated worldwide via various telecommunication channels. In addition these elements are tuned so that the user will recover the orbit in an optimal way. So-called tuned IRVs (Inter-Range Vectors) and tuned SAO-elements (Smithsonian Astrophysical Observatory) are delivered to the SLR community, PRARE-elements to the PRARE system.

### 3. Tuning

The orbit is recovered at the SLR sites by simple programs intended for use on low capacity computers. These programs adopt low degree and order gravity fields and do not consider nongravitational forces as drag. The IRVINT integrator written at the university of Texas starts from the IRVs. The ancient AIMLASER program applies analytical orbit theory to recover the orbit from the SAO-elements.

Because of these severe neglects, D-PAF tunes IRVs and SAO-elements. This means that despite of simple perturbation modelling onsite the orbit is recovered in an optimal way. The optimum is a minimum difference in the least squares sense of the recovered orbit to the full perturbation model orbit or reference orbit. The IRVINT and AIMLASER programs have to run then in a defined mode. D-PAF assumes for IRVINT a 60s integration step size and the GEM10N gravity field coefficients up to degree and order 18. The AIMLASER program should run in the RGO version (Royal Greenwich Observatory) with dedicated GEM10B coefficients.

Fig. 1 shows the along-track error if an un-tuned IRV is integrated by IRVINT. The example holds in general. Due to the missing drag forces modelling the error grows during the day to ca. 1400m in along-track position or ca. 200ms in time bias which would prevent tracking of the satellite.

Fig. 2 displays the error after tuning. Maxima are now ca. 20ms around midnight and around noon. The remaining along-track errors are similar day by day, the maxima are dependent on the solar activity. They could be accounted for by a function giving the error for 24 hours of a day. The more proper way of course would be to model drag in the integrator. Anyway the remaining errors are in a range that can be accepted for tracking.

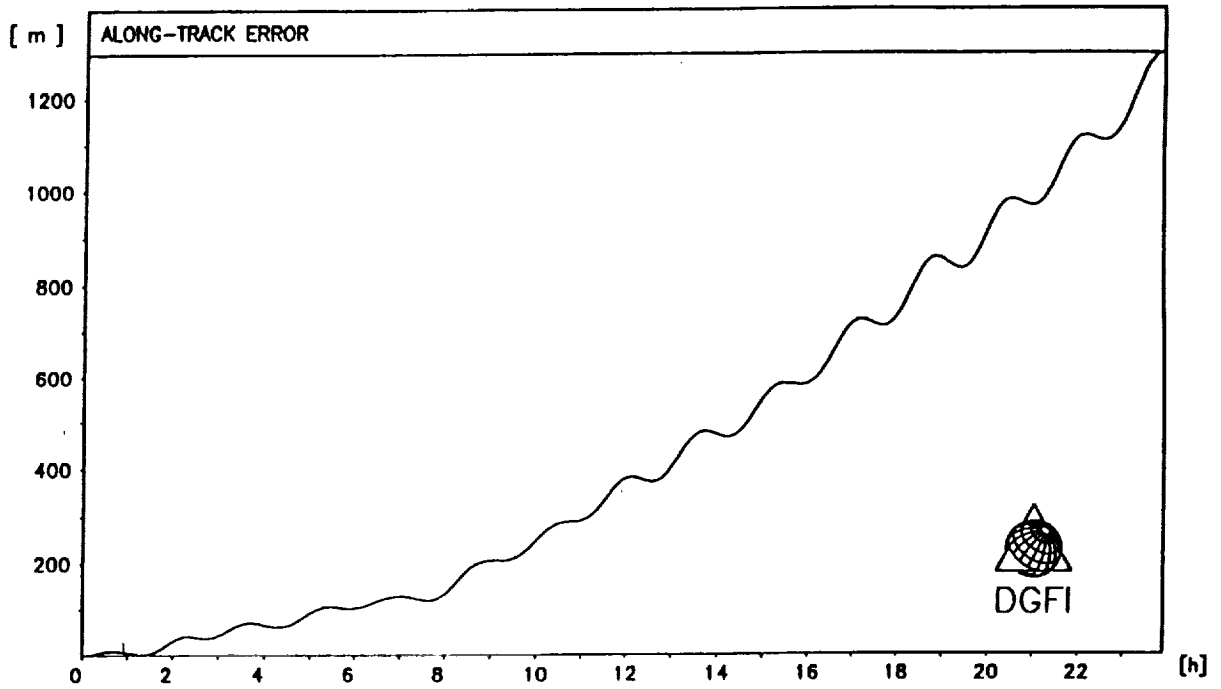


Figure 1 Along-track error from un-tuned IRVs

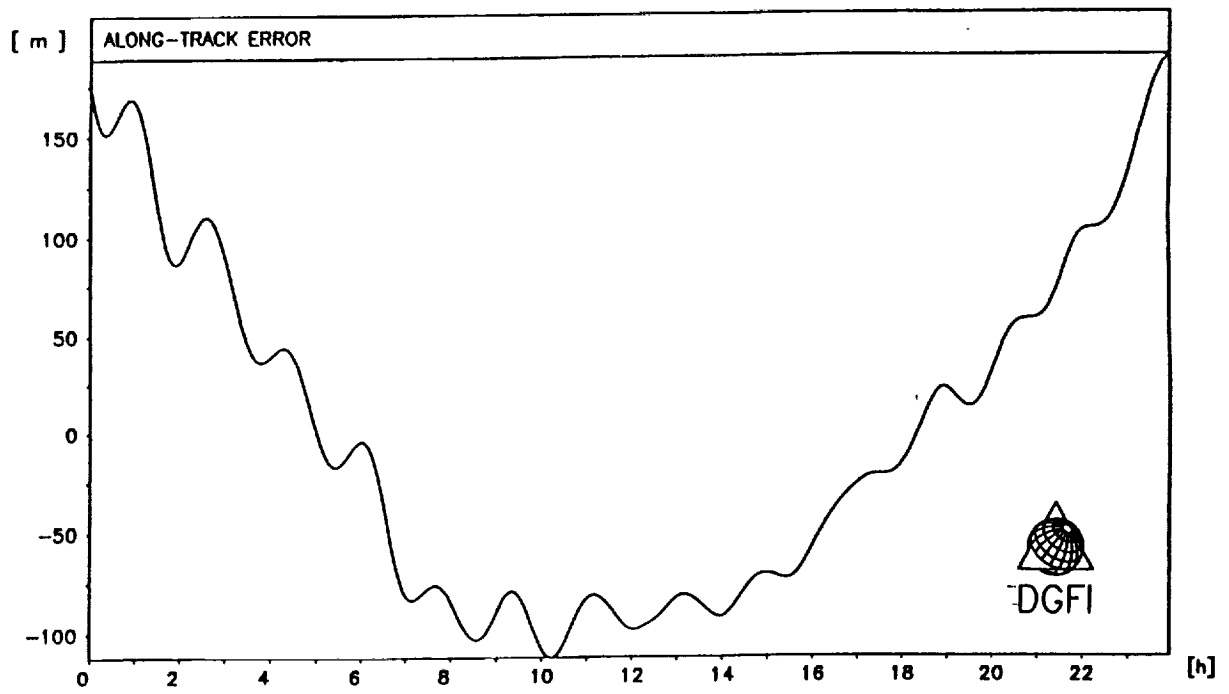


Figure 2 Along-track error from tuned IRVs

The accuracy of tuning, that is the difference of the recovered orbit to the reference orbit, can be seen in Table 1 where the typical differences are given as RMS-values in meters for both types of prediction elements. Again the values are largely dependent on the solar activity.

	IRVs 1d	SAO-elements 10d
radial	3-5	10-20
across-track	3	10
along-track	20-60	20-100

Table 1: Tuning accuracy (in m)

The SAO-elements show less accurate recovery because they represent the whole prediction period (normally 10d) whereas the IRVs are given each day. All values are within a range that can be accepted for tracking.

#### 4. Time Bias

D-PAF generates and disseminates weekly prediction sets containing IRVs and SAO-elements. Due to the sensitivity of ERS-1 to variations of the high atmosphere the predictions loose accuracy mainly in along-track direction. This is also known to the stations as so-called time bias i.e. the satellite rises too late or the satellite rises too early. The determination of the time bias provides a quick and simple update of the orbit predictions.

Therefore D-PAF generates and disseminates daily a time bias function from new Q/L (Quick Look) Laser ranges. For every pass over all stations having observed ERS-1, a time bias is computed relative to the last prediction set. A third order function in time is fitted by LS (Least Squares) to these time bias values. In the LS procedure the time bias values are checked for outliers and the parameters are checked for significance leading all in all to a best approximating function. The function fits to the time bias values within 1ms for up to four days.

A typical example of time bias values is given in Fig.3. Fig.4 shows the fitted function after removing the outliers and after the significance check of the parameters.

The time bias function represents the time bias values of the last few days. More important it is capable of predicting the along-track error.

The EDC (European Data Center) provides another important tool to handle the time bias problem. Stations can store the observed time bias immediately after the pass in the data base. Currently Graz, Potsdam, RGO, Santiago de Cuba and Wettzell do so. This time bias is nearly in real-time available to other stations. The stations can then compare the results with their own computations and with the D-PAF time bias function. This all this together should yield to more confidence in the time bias that is going to be used for the next upcoming pass.

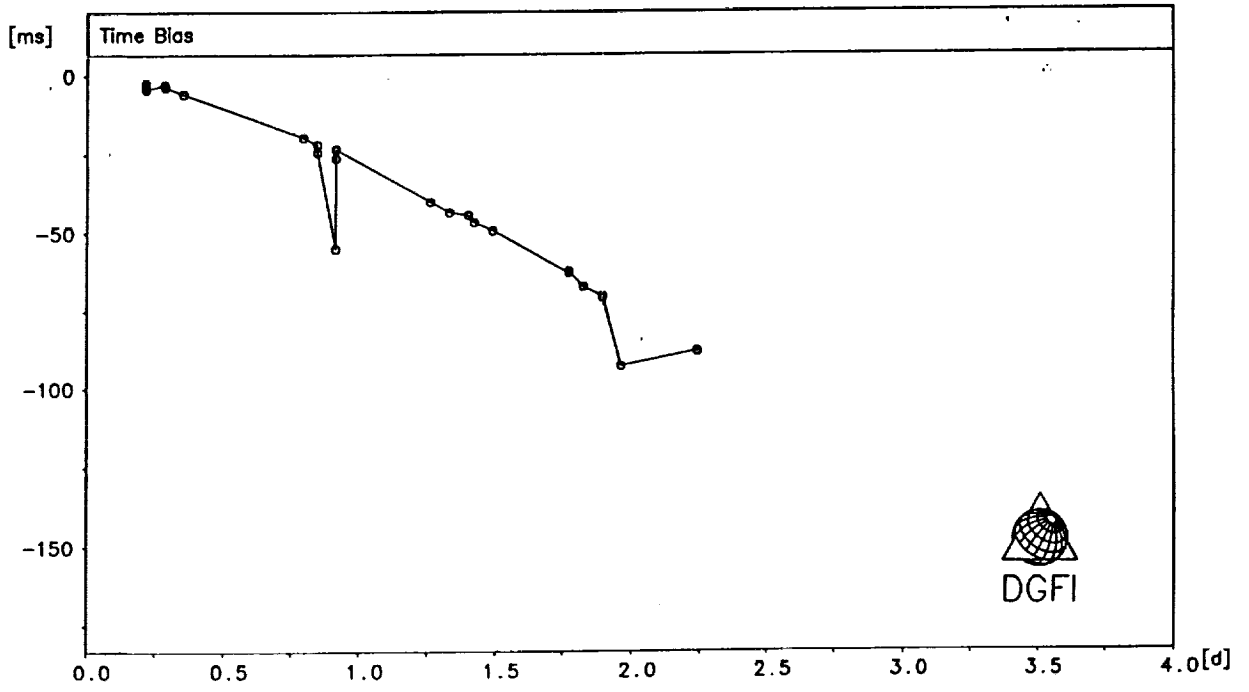


Figure 3 Time bias values

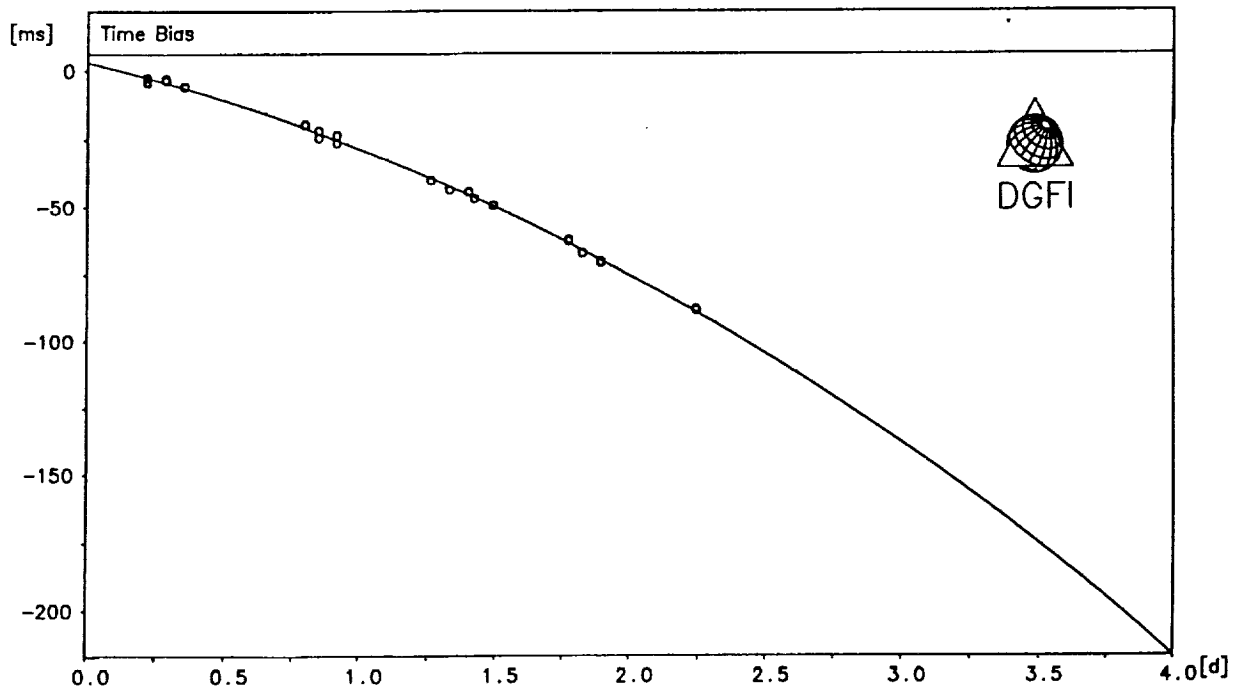


Figure 4 Time bias function



## 5. Quality

The quality of the ERS-1 prediction products is indicated to the users by a quality flag. In case of orbit predictions the quality flag is computed from the fit of observations in the orbit analysis (step 1 in chapter 2), from the comparison of overlapping arcs and from the tuning accuracy. The quality of the time bias function is assessed from the approximation error of the function and the data coverage.

Of course the quality flag gives only an idea on how the quality of the products can be. By nature predictions go into the future and nobody can determine what will be. Particularly the accuracy of ERS-1 orbit predictions is heavily influenced by unpredictable solar activity. Anyway the quality flag shows the current knowledge of the quality. It convinces the generator that he did a good job and it gives a first indication to the user in case he has problems.

All prediction products are subject to permanent quality checks. Daily the time bias of newly incoming Q/L Laser passes are determined relative to the actual prediction orbit which leads to the time bias function. The prediction orbit is also compared to the MMCC orbit (Mission and Management Control Center). The MMCC orbit is generated by an independent group in ESOC (European Space Operation Center), Darmstadt, from S-band observations and radar altimeter fast delivery ranges. The comparison with such a completely external source provides more confidence in the results.

On a weekly basis when new orbit predictions are generated the new prediction orbit is compared to the old one. The differences in along-track direction should exactly reflect the old time bias function. The differences in radial and across-track direction normally stay within a few meters.

The internal quality checks proceed in a closed loop from prediction set to prediction set. The external checks give an independent judgement. So the reliability of the orbit prediction system has reached a quite high level.

Fig.5 displays the along-track errors of ERS-1 orbit predictions since launch. The first 100d are clearly affected by large solar activities. In addition a manoeuvre was missed. Meanwhile these cases are taken care of. In the right half of Fig.5 it can be seen that the mean accuracy steadily improves, but is clearly degraded by the frequent manoeuvres.

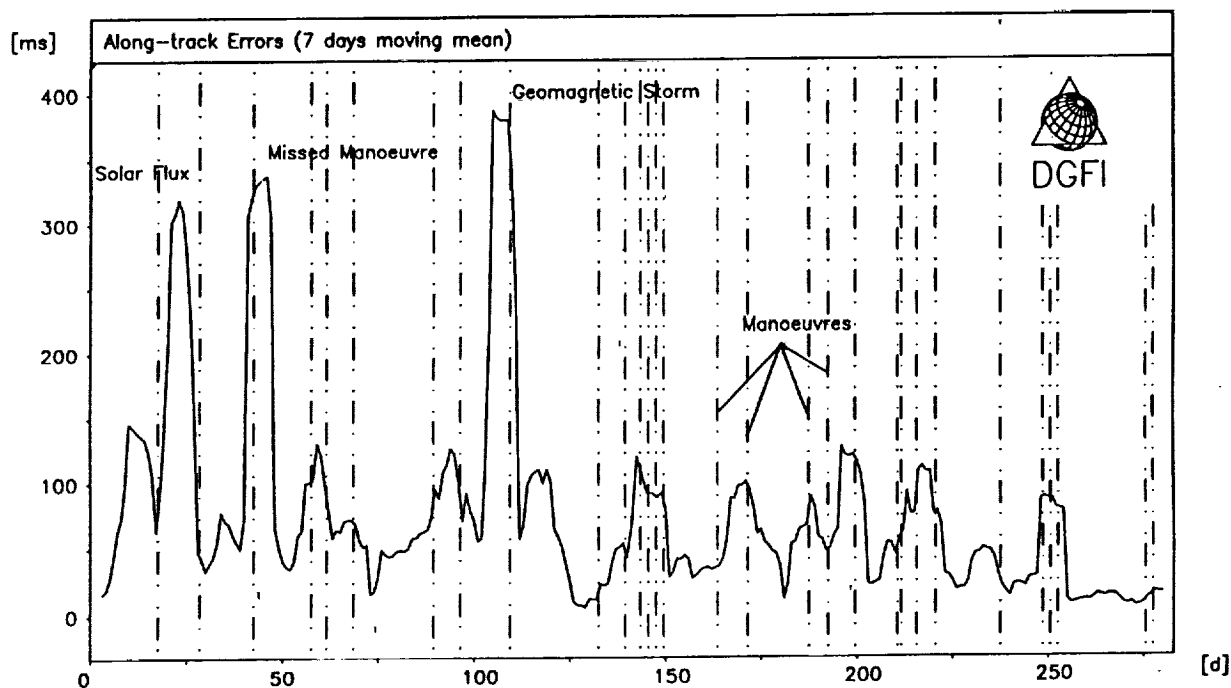


Figure 5 Accuracy of ERS-1 orbit predictions

## 6. Conclusions

It has been shown that tuning of orbit predictions is essential for ERS-1. D-PAF provides daily time bias functions that account for the along-track error of the predictions. The quality of ERS-1 prediction products is assessed and indicated to the users. The predictions are permanently checked internally and externally. The average accuracy has considerably improved since launch.

## 7. Literature

Massmann, F.-H., Reigber, Ch., Li, H., König, R., Raimondo, J.C., Rajasenan, C. and M. Vei: *Laser Ranging Network Performance and Routine Orbit Determination at D-PAF*, this proceedings

Schwintzer, P., et. 14 al.: *GRIM4 - Globale Erdschwerefeldmodelle*, Zeitschrift für Vermessungswesen 117, pp. 227-247, 1992

COMPENSATION FOR THE DISTORTION IN SATELLITE LASER RANGE  
PREDICTIONS DUE TO VARYING PULSE TRAVEL TIMES

Matti Paunonen

Finnish Geodetic Institute  
Ilmalankatu 1A  
SF-00240 Helsinki, Finland  
Telefax:358-0-264995

ABSTRACT

A method for compensating for the effect of the varying travel time of a transmitted laser pulse to a satellite is described. The "observed minus predicted" range differences then appear to be linear, which makes data screening or use in range gating more effective.

1. INTRODUCTION

Accurate range predictions are necessary in satellite laser range measurements when the operation takes place in daylight. Then the range gate, where the return pulse detector is active, can be set very narrow to effectively discriminate against noise. Data screening of the observations is often done using "observed minus predicted" (O-C) range differences. The predicted satellite times are generally equally spaced, as are the transmit times. But the true hitting times are not equally spaced because of the varying pulse travel times. This leads to distortion of the O-C differences which can be as high as 10-20 m. A polynomial of suitable degree is used in screening. It is well known that the polynomial should be of low degree so as to avoid an artificially good fit or end effects. If the travel time distortion is removed, the O-C deviations are nearly constant with time for high quality orbit predictions. This paper describes and tests a simple correction method.

## 2. METHOD OF RANGE CORRECTION

The range from the laser station to the satellite varies approximately parabolically with time, Fig. 1. When the satellite is passing the closest point, a small time change does not affect the range much. At the far end of the pass the range changes several kilometers per second.

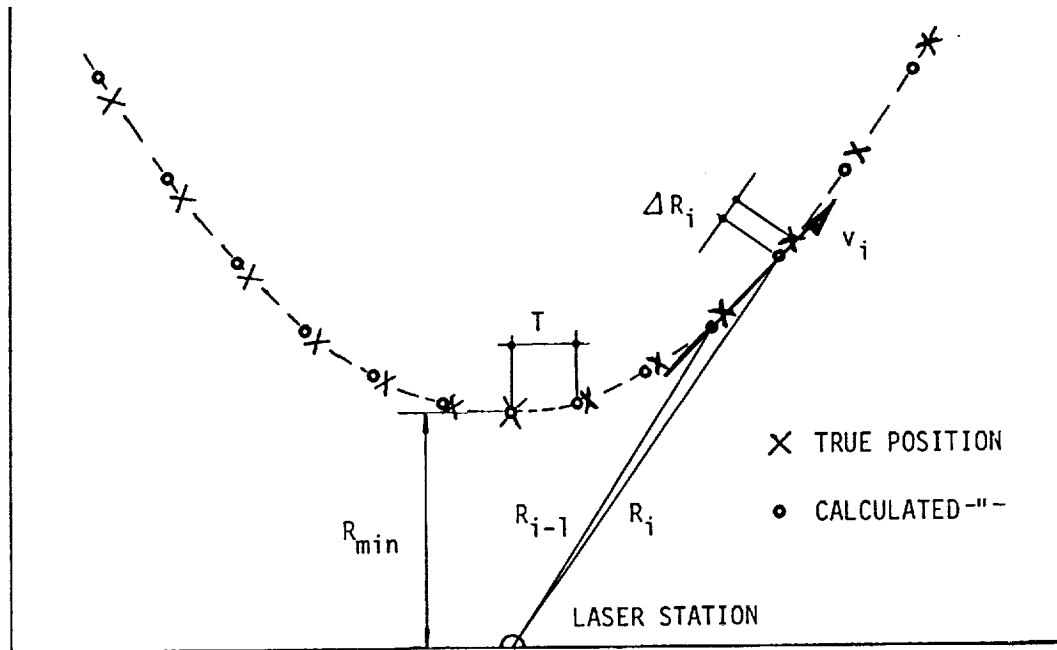


Fig.1 Conceptual scheme for the origin of the travel time distortion in ranges.

This rate,  $v_i$ , can be calculated together with the ranges, or it can be approximated from the change between the successive predicted ranges  $R_{i-1}$  and  $R_i$

$$v_i = (R_i - R_{i-1}) / T, \quad (1)$$

where  $T$  is the time step (often 1 s).

The travel time difference between the minimum range  $R_{min}$ , and the instantaneous range  $R_i$  is

$$\Delta t_i = (R_i - R_{min}) / c, \quad (2)$$

where  $c$  is the speed of light. Then the travel time correction  $\Delta R_i$  to be added to the predicted range is

$$\Delta R_i = v_i * \Delta t_i. \quad (3)$$

### 3. RESULTS AND DISCUSSION

A test with real data is shown in Fig. 2. This LAGEOS pass involved relatively few observations (21). The prediction program used highly accurate long-term IRV predictions /1/. A 220 ms time correction was used in the calculation.

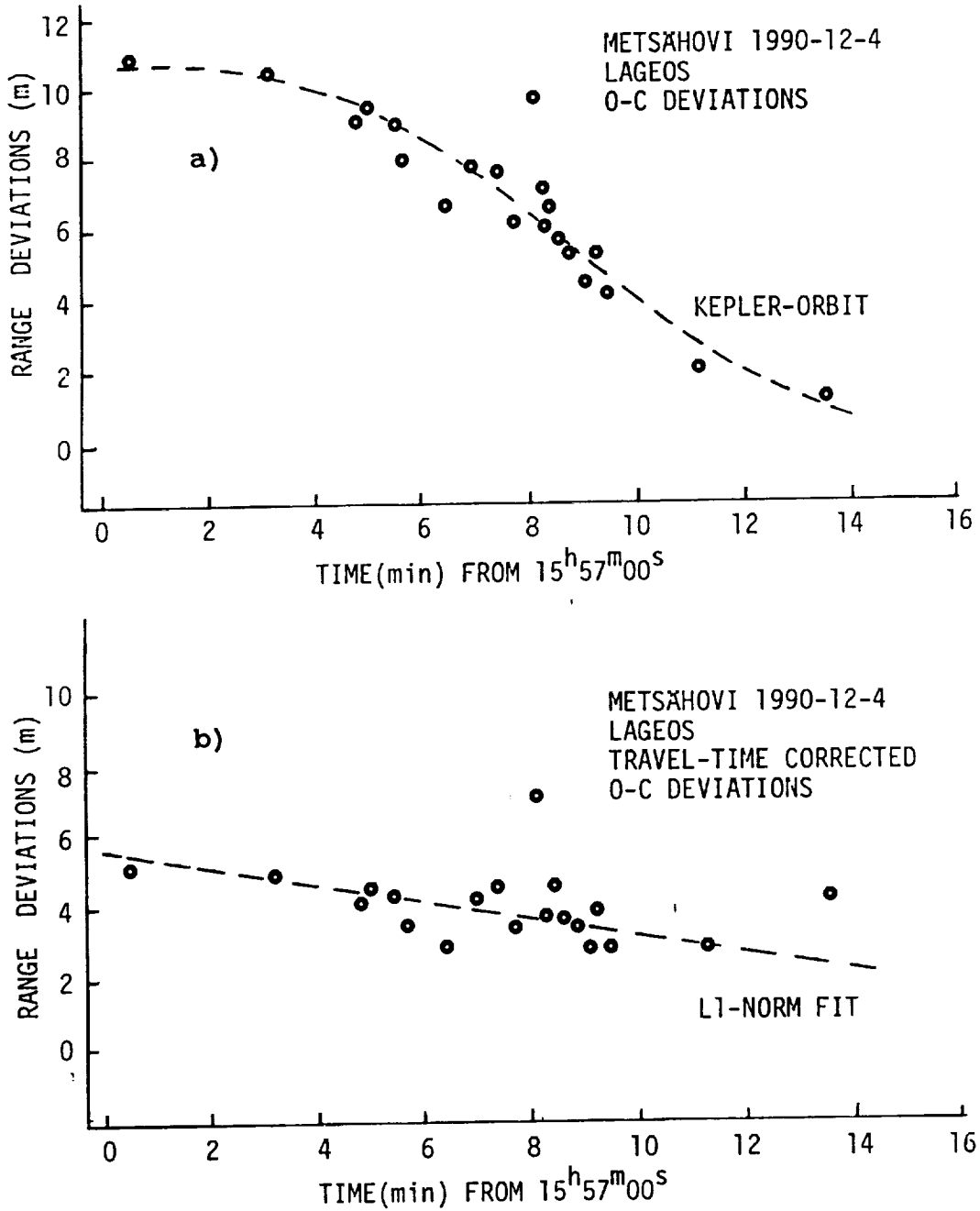


Fig. 2. a) 'Observed-predicted' (O-C) deviations of a measured LAGEOS pass. A Kepler orbit fit is also shown. b) O-C deviations after the travel time correction. A linear median fit is shown.

The time error varies slowly with time, and is normally known from earlier observations. The O-C deviations are shown in Fig. 2a. A simple Kepler orbit /2/ fits the observations quite well, and only one outlier is indicated. In polynomial fitting determination of the order is not easy. The first point would be rejected in a linear fit.

The situation becomes considerably clearer after application of the travel time correction method described (Fig.2b). The fit using the linear L1-norm /3/ eliminated the last point as well as the known outlier. Because the model is now linear, it is not necessary to use higher order polynomials.

This example shows that a very narrow range window is possible in ranging to LAGEOS. A 50 ns window corresponds to 7.5 m of range. This would help considerably in implementing daylight satellite laser range-finding. As has been seen, the method can also help resolve difficult data screening tasks. Good orbit elements and a good orbit are essential for this method.

Note that recalculation of the orbit after the pass, using the satellite hit times, produces approximately the same O-C deviations as the method described.

#### REFERENCES

1. The Texas University, long term IRV- predictions for LAGEOS satellite; a satellite prediction program ORBIT developed at the Royal Greenwich Observatory, Herstmonceaux, England.
2. J. Kakkuri, O. Ojanen, M. Paunonen, Ranging precision of the Finnish satellite laser range finder. Reports of the Finnish Geodetic Institute 78:8, Helsinki 1978, 11 p.
3. M. Paunonen, Use of the L1-norm in screening laser range observations to satellites. Proc. 18th Inter-cosmos Symposium on the Use of Artificial Satellite Observations for Geodesy and Geophysics, June 12-17, 1989, Cracow, Poland (Ed. Wl. Goral, Observations of Artificial satellites of the Earth, No 27, 1989, Polish Academy of Sciences, Warsaw 1990), pp.359-362.

## Timebias corrections to predictions

Roger Wood and Philip Gibbs

Satellite Laser Ranger Group  
Herstmonceux Castle, Hailsham  
East Sussex, BN27 1RP, UK

*Abstract This talk aims to highlight the importance to an SLR observer of an accurate knowledge of the timebias corrections to predicted orbits, especially for low satellites. Sources of timebias values and the optimum strategy for extrapolation are discussed from the viewpoint of the observer wishing to maximise the chances of getting returns from the next pass. What is said may be seen as a commercial encouraging wider and speedier use of existing data centres for mutually beneficial exchange of timebias data.*

### Introduction

The real behaviour of low satellites is never in exact agreement with even the best predictions. The principal reasons are that modelling the effect of atmospheric drag is difficult, and the perturbations due to solar radiation pressure are not predictable in advance. ERS-1 is much larger and somewhat lower than either Starlette or Ajisai and consequently presents the biggest headaches in making predictions. Despite the problems, detailed elsewhere in these proceedings, the prediction teams do an excellent job in providing orbits and thereby give observing stations the best possible chance of tracking the satellites successfully. Fortunately, most of the deviation from the predicted orbit appears as an along-track error and can be corrected by applying a suitable timebias to the predictions (as has been done very successfully for Lageos for many years now). For a particular set of predictions observing stations can, for each satellite, model the history of the behaviour of the timebias with time and extrapolate to predict the timebias at the time of observation of the next pass.

At Herstmonceux we have been working to improve the accuracy of our extrapolation of timebias values. This talk outlines our findings, indicates the benefits to be gained from increased use of the data centres and shows how helpful good timebiases can be if you have English weather and are trying to keep us with Grasse!

### Why do we need accurate timebiases?

We see three distinct advantages:

**Ease of satellite acquisition.** This is always important, at whatever stage of the pass the satellite is first acquired. But it is especially important at the very beginning of a pass, necessarily at low elevation, when accurate pointing helps to minimise the time spent in searching for returns. Ease of acquisition is also important when there has been a break of a few days in the sequence of observations, because of cloud or technical downtime, where accurate knowledge of the timebias correction can lead to immediate recovery of the satellite. This second point emphasises the usefulness of having access to continuous records of timebias data in order to base any extrapolation on the best available data set.

**Improved telescope tracking.** If an incorrect timebias is used to compute the telescope position during a pass, the offsets from the reference position on the detector will depend on time and the observer will have to insert ever-changing manual corrections in order to keep the satellite image. By contrast a correct timebias results in little or no guiding, provided that the pointing model for the telescope is well-determined.

**Better noise elimination.** When the timebias is exactly right the returns from the satellite always appear at the same place in the range window. This means that the window can be made very small and so the amount of noise reaching the detector can be drastically reduced. This improvement in the ratio of signal to noise is particularly valuable for daylight ranging.

The second and third advantages can still be gained (even in cases where an accurate timebias is not available beforehand) if the first few good returns from the satellite are used in real time to convert a range offset into a timebias correction. This technique is routinely applied for multi-photon detection systems where the identity of true returns is not in doubt. But for single photon detection in daylight, or using an intrinsically noisy detector such as a SPAD, it is not always easy for the software to pick out the track, and some form of manual intervention may be required.

### Where can we get timebiases?

Originally we used only our own history of passes to make extrapolations to current behaviour. This was quite satisfactory during periods of continuous good weather, but was often very frustrating when trying to recover satellites after a break of two or three days due to cloud or instrumental problems.

Then, for Ajisai and Starlette, we tried using Bendix's timebias data from many stations in addition to our own. We immediately found a great improvement in the quality of our extrapolation and could use narrower range windows right at the start of the pass. We also found that the change from using elements to using IRVs gave better consistency in the timebias histories.

When ERS-1 was launched we, like everyone else, had mixed success in finding it. When we had a reasonable history and the solar activity was not too wild, we got good passes. But at other times, once we had failed to get passes for a day or two, it became increasingly difficult to recover the satellite. We were very pleased when DGF1 agreed to use the pass data that they receive from many stations to produce timebias functions for ERS-1. This gave, and continues to give, valuable additional weight to timebias trends.

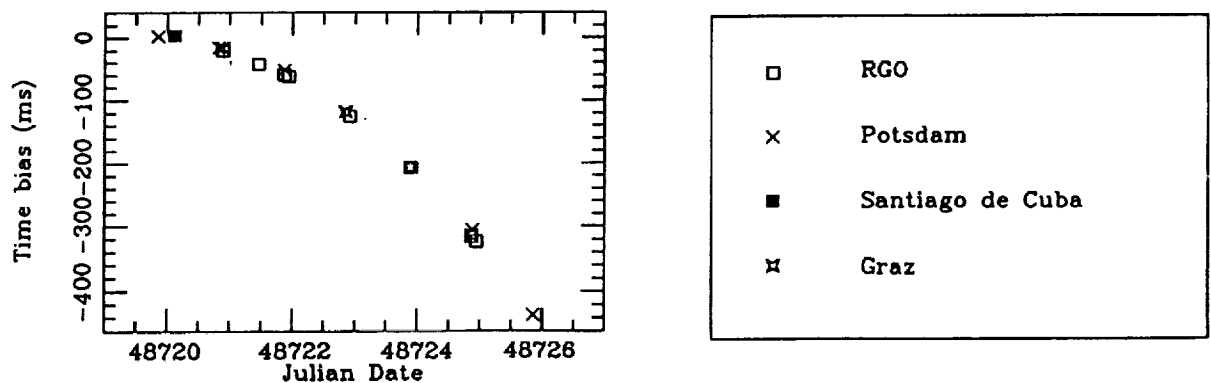


Figure 1: ERS-1 timebiases from EDC for IRV set A920407 and symbol key



Since then, following the establishment of the European Data Centre (EDC), a small number of stations have begun to make regular deposits of their timebias data for ERS-1 soon after the observations. We often get EDC data from Graz and Potsdam—and occasionally from Wettzell and Santiago de Cuba. Figure 1 shows a plot of the data deposited for IRV set A920407 at the beginning of 1992 April. The interagreement between the values from different stations is striking and gives great confidence that all timebiases have been reduced to a common system. But, with all the stations close together in Europe, it is clear that the data are clumped together in time: indeed, sometimes they are all clouded out simultaneously! The addition of more data points from other stations at other longitudes around the world would give much better “round the clock” coverage.

### How can we best use timebias histories?

**ERS-1** Over the last two or three months we have been investigating how best to predict future timebias values from whatever timebias history we had available on a particular day. This usually consisted of a small number of values covering a few days.

First we looked at the timebiases shown in Figure 1 which cover a period of about a week and are all referred to the same IRV set from DGFI. Our approach was to see, in retrospect, how well the observed values available up to a certain day could be used as predictors for the points which followed. The results of our trial fits are shown in Figure 2. First we fitted to data for the first two days only; next we used data for the first three days; then the first four days and so on. For each

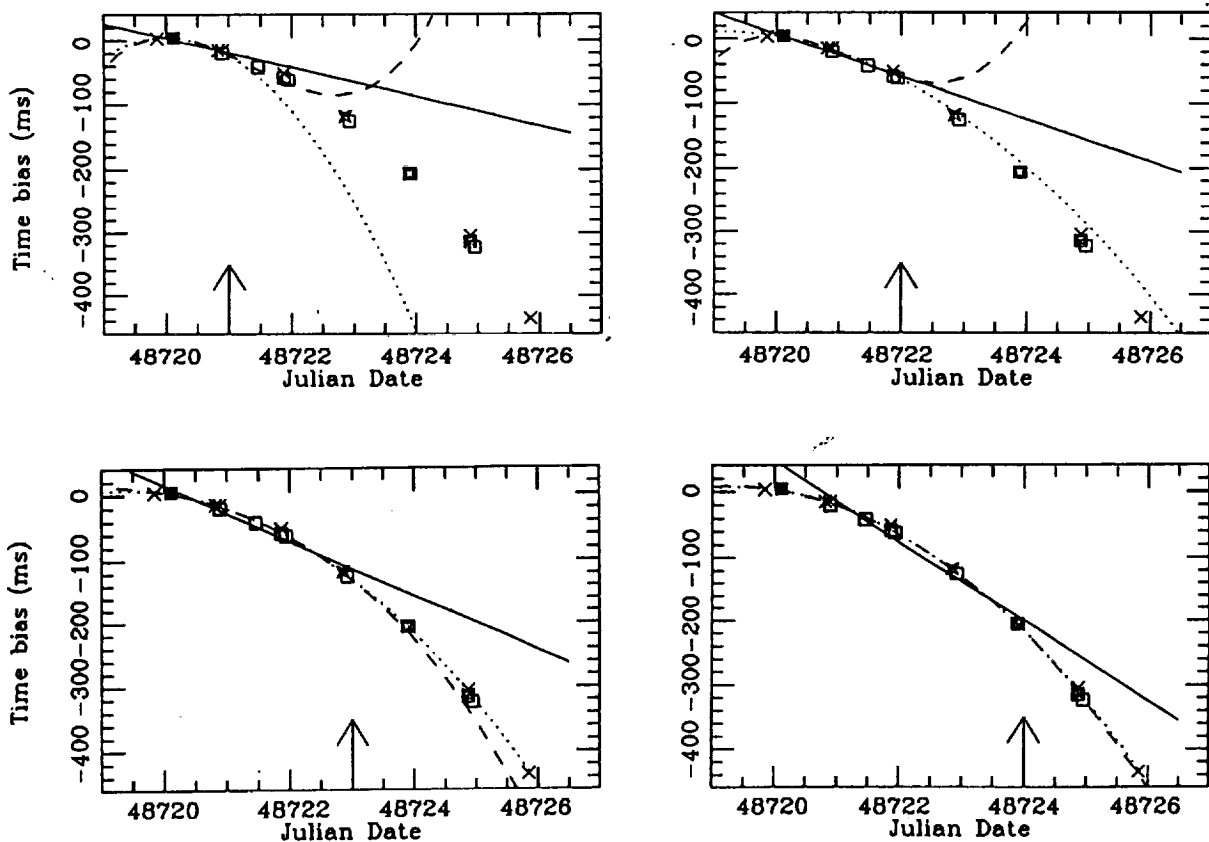


Figure 2: *Successive fits to ERS-1 timebiases from EDC*

trial we fitted the data with functions of three different orders—linear (represented by a solid line in Figure 2), quadratic (dotted line) and cubic (dashed line). Only points to the left of the vertical arrow at the bottom of each plot were included in the fit. We then looked at the next few points to the right of the arrow to see how well, or how badly, each of the attempted fits represented the data which followed. From this examination we drew a number of preliminary conclusions:

- Use the simplest function which gives a *reasonable* fit to the data (even if it is not the *best* fit)—it will generally be better for extrapolation than a higher order function;
- Use only linear fits for the first 2 or 3 days—there are too few data points to justify anything fancy;
- It would be helpful to have quick timebias deposits by all stations and better longitude coverage. This would:
  - fill the gaps in the European data;
  - add data points to strengthen the fit;
  - provide actual timebias values closer to the time of observation than are available now.

More recently we tried a new experiment based on normal point data for ERS-1 passes extracted from the CDDIS database and reduced to give timebiases. [We had hoped to use directly the Bendix values, but there are currently unexplained discrepancies between their derived values of timebias and ours, so we have worked entirely from the normal point data. This effect also appears to exist in the Bendix timebiases for Ajisai and Starlette, but to a lesser extent which does not prevent their use in revealing long-term trends]. In this case we took the data set shown in Figure 3 which covers a week in early May and is referred to IRV set A920505 from DGFI. It is clear that

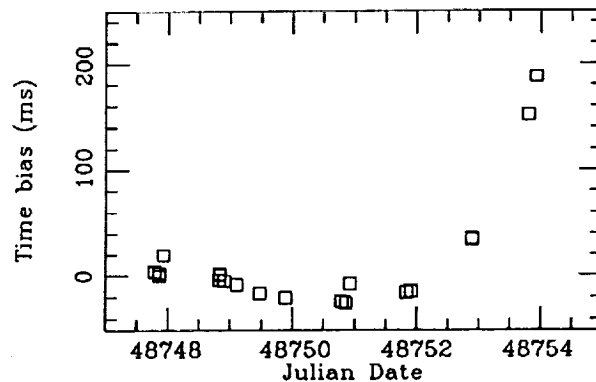


Figure 3: *ERS-1 timebiases from CDDIS normal points*

the longitude coverage is more uniform and the daily density of points is higher. However, there is a drawback as far as immediacy is concerned in that the turn round time for data input can be longer than for EDC, so that some of the data are relatively old. We then followed the same procedure that we used for the EDC data and made trial fits to subsets of the data to see how well the extrapolated curves acted as predictors for what was subsequently observed. The plots in Figure 4 again show that the higher order fits are wildly ineffective for the first few days, and only begin to make more sense later. But around day 48752 the data take a wholly unexpected turn towards large positive values and the trends evident in the early points are no longer relevant. This sudden change of behaviour is probably due to solar activity, and in such circumstances it is wise to abandon the early points of the data set and start the fit again from part way through.

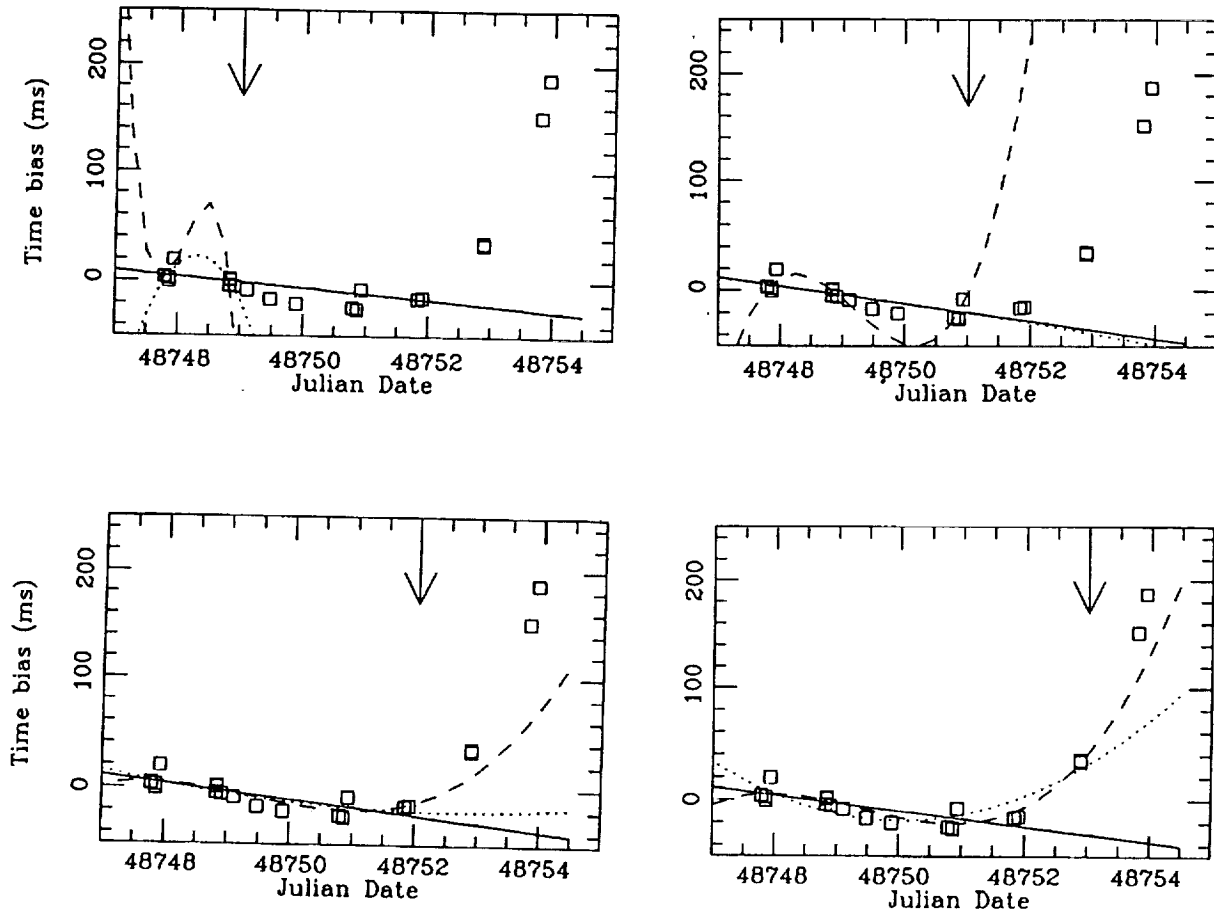


Figure 4: *Successive fits to ERS-1 timebiases from CDDIS*

Our additional conclusions as a result of this exercise were:

- For ERS-1 it is necessary to examine the data and functions daily in order to pick up unexpected trends in good time;
- Better longitude coverage is essential for early warning of departures from previous behaviour;
- Access to the raw data is very useful for making value judgements on the quality of the fit of any functions!

**Ajisai and Starlette** Generally the prediction of timebiases for these satellites is much more straightforward than for ERS-1 since they are relatively unaffected by atmospheric drag and solar radiation pressure. Indeed orbit predictions can run quite satisfactorily for several weeks so that a long timebias history can be established for one IRV set. Over such an interval timebias corrections usually behave sensibly and, even when the corrections get quite large, a good history with respect to one set of IRVs allows meaningful extrapolation to get accurate values.

### What can be done to improve?

We think that all stations can share the clear benefits to be gained from the daily examination of trends in timebiases for ERS-1 by depositing their timebias values with data centres as soon as possible after the pass has ended. Then, by retrieving a comprehensive set of timebiases obtained

worldwide, and using it as the basis for extrapolation, the "hit rate" can be significantly improved. Alternatively, but probably with greater delay, stations can retrieve normal point data and derive timebiases from them.

It would be very worthwhile to extend the system to include Ajisai and Starlette; and to make sure that provision is made for rapid feedback of Topex/Poseidon data.

Finally the proper commercial: we think that timebiases are just like washing powder—use the right one and your whole life is transformed for the better!

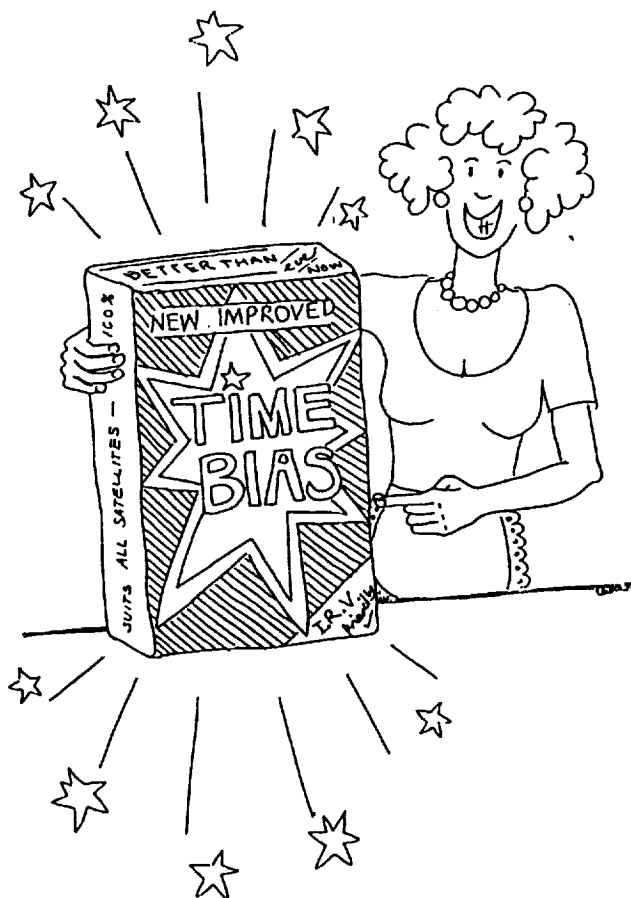


Figure 5: "New improved Timebias"

### Acknowledgements

We wish to thank the staff of the prediction and data archiving centres for advice and data. Special thanks go to Brion Conklin of Bendix for his speedy and cheerful responses to our many requests. We greatly appreciate assistance from Rolf Koenig of DGFI and Wolfgang Seemüller of the European Data Centre.

## Formation of on-site Normal Points

G.M. Appleby and A.T. Sinclair  
Royal Greenwich Observatory  
Madingley Road  
Cambridge CB3 0EZ, UK

### Abstract.

*We describe our methods of fitting a smoothing function to observational range differences from a predicted orbit, by deducing corrections to the orbit in the radial and along-track directions. The method has been used on observations of a variety of satellites, and using predicted orbits computed both by numerical integration using IRVs as starting values and analytically from orbital elements. The along-track corrections to the predicted orbit have been successfully used in the form of time biases to improve subsequent predictions, and a statistical test has been devised to ensure that the range residuals may be used to form unbiased quicklook normal points.*

### 1. Introduction.

It was recommended at the Fifth International Laser Ranging Instrumentation Workshop held at Herstmonceux, UK, that laser range normal points should be formed by the stations shortly after each satellite pass and transmitted as quicklook data (Gaignebet, 1985). The final version of the quicklook normal point format was agreed by the SLR Subcommittee of the CSTG and published in the April 1990 Satellite Laser Ranging Newsletter (Schutz, 1990). The process of forming normal points consists of 2 stages; (a) fitting a smoothing function to the observational range differences from a predicted orbit and subtracting the function in order to form a flat track of residuals, and (b) rejecting noise and outliers and forming the mean values of the accepted residuals in bins spread through the pass. The values of the smoothing function and the predicted orbit at the epoch of an actual observation nearest the mean epoch of the bin are then added to the mean value of the residuals in the bin. The resulting normal points are then virtually independent of both the smoothing function and of the predicted orbit.

In this report we detail the processes adopted to carry out stage (a) of the process; methods for rejecting noise and forming unbiased normal point bin means are developed by Sinclair (these proceedings)

### 2. Development of the Smoothing Function.

During the observation of a satellite pass, differences from the predicted range are computed for all events detected within the range gate and displayed in realtime, true satellite returns appearing as a track of correlated values among the randomly distributed noise events. An example of such a plot is given in Figure 1, which shows a pass of ERS-1. The rejection of gross noise events is carried out visually using the plot, and the subsequent set of satellite

range measurements and some noise events are passed to the next stage of processing.

At an early stage of the development of the preprocessing software, the decision was taken to use the pass-by-pass observations to solve for corrections to the predicted orbit, and in particular to monitor the along-track error, in order to improve subsequent prediction accuracy. Thus the possible use of an arbitrary polynomial for the smoothing function was not considered. However, corrections to the predicted orbital elements of the satellite would be difficult to apply to orbits computed by numerical integration and using IRVs as starting values, and similarly corrections to the IRVs would not be applicable to orbits computed analytically. Thus it was decided to express orbital corrections as along-track, across-track and radial displacements to the predicted position. Such corrections are then readily applied to the geocentric orbit during the solution iteration process, and the derived along-track correction can be expressed as an orbital time-bias for improving subsequent predictions.

During the prediction process an orbit in the form of geocentric rectangular satellite coordinates and velocities at 1-minute time intervals and in units of Mm and Mm/day, is computed and stored. For each observational epoch, we use 8th order Lagrangean interpolation to compute the instantaneous position  $\mathbf{r}$  and velocity  $\mathbf{v}$  of the satellite. Let  $\mathbf{r} = (x, y, z)$ , and  $\mathbf{v} = (v_x, v_y, v_z)$ , and let the magnitudes of these vectors be  $r$  and  $v$  respectively. The reference frame used is different depending upon the source of the orbit being considered; for an orbit generated by numerical integration and using IRVs, the coordinates are given with respect to the true equator and mean equinox at 0hrs UT of the epoch of the IRVs. For an analytically-derived orbit, the coordinates are given with respect to the mean equator and equinox of date. At the observational epoch, we compute the coordinates of the observing station in the same reference frame. Let the station coordinates be  $\mathbf{s} = (x_s, y_s, z_s)$ . Then the predicted topocentric coordinates of the satellite are

$$x_T = x - x_s, \quad y_T = y - y_s, \quad z_T = z - z_s \quad ,$$

and the predicted range is the magnitude of this topocentric vector. We thus form the difference of the observed from the predicted range, and in order to solve for corrections to the predicted orbit we require partial derivatives of range with respect to the along-track, across-track and radial components of the displacement of the predicted orbit.

## 2.2 Partial Derivatives.

(a) Let the along-track displacement or time-bias be  $\Delta T$ .

Then the displaced range  $R$  is given by

$$R^2 = (x + v_x \Delta T - x_s)^2 + (y + v_y \Delta T - y_s)^2 + (z + v_z \Delta T - z_s)^2$$

Then

$$R \frac{\partial R}{\partial \Delta T} = v_x(x + v_x \Delta T - x_s) + v_y(y + v_y \Delta T - y_s) + v_z(z + v_z \Delta T - z_s),$$

or approximately

$$\frac{\partial R}{\partial \Delta T} = (v_x x_T + v_y y_T + v_z z_T)/R$$

(b) Let the across-track displacement be  $\Delta Q$

The across-track direction is

$$\frac{\mathbf{r} \times \mathbf{v}}{\mathbf{r} \cdot \mathbf{v}} = (l, m, n) \quad , \text{ say.}$$

So,

$$l = (y v_z - z v_y)/rv$$

$$m = (z v_x - x v_z)/rv$$

$$n = (x v_y - y v_x)/rv$$

So the displaced range  $R$  is given by

$$R^2 = (x + l\Delta Q - x_s)^2 + (y + m\Delta Q - y_s)^2 + (z + n\Delta Q - z_s)^2$$

So,

$$R \frac{\partial R}{\partial \Delta Q} = l(x + l\Delta Q - x_s) + m(y + m\Delta Q - y_s) + n(z + n\Delta Q - z_s),$$

or approximately

$$\frac{\partial R}{\partial \Delta Q} = (l x_T + m y_T + n z_T)/R$$

(c) Let the radial displacement be  $\Delta r$

So the displaced coordinates of the satellite are  $x + x\Delta r/r$ , etc.

So the displaced range  $R$  is given by

$$R^2 = (x + \frac{x\Delta r}{r} - x_s)^2 + (y + \frac{y\Delta r}{r} - y_s)^2 + (z + \frac{z\Delta r}{r} - z_s)^2$$

Then as before we calculate the approximate partial derivative

$$\frac{\partial R}{\partial \Delta r} = (x x_T + y y_T + z z_T)/(rR)$$

### 2.3 Solutions.

In practice it was found that the across-track correction was always highly correlated with the radial correction, and in many cases the solution was indeterminate. Hence both could not be solved-for, and so it was decided to suppress the solution for across-track, and solve for a radial correction only, which would thus absorb the across-track error. It was also found that simple constant along-track and radial corrections to the predicted orbit did not in general absorb all the error in the orbits, and that the set of parameters to be determined for a particular pass should be selected from along-track and radial displacements and their time rates of change and accelerations. We denote these parameters  $T, \dot{T}, \ddot{T}, R, \dot{R}, \ddot{R}$ . The partial derivatives of range with respect to the rates of change and accelerations of these parameters were formed from those of the constant terms by multiplication by  $t$  and  $t^2$ , where time  $t$  is the epoch of each observation relative to the mid-time of the pass. Such a definition for the origin of  $t$  is optimum in reducing correlations between the unknowns. It was usually found necessary to solve for only 4 of the possible six parameters, but occasionally all six were required to remove all trends from the observational residuals.

Initially a scheme was devised to automatically check for very high ( $>0.999$ ) correlations among the 4 unknowns  $\dot{T}, \ddot{T}, \dot{R}, \ddot{R}$ , and to suppress any one or two of them in order to obtain a determinate solution, consistent with obtaining a flat track of residuals. However experience showed that the values determined for these 4 parameters were always quite small, of the order of 0.1 ms/minute for  $\dot{T}$  and 1.0 cm/minute for  $\dot{R}$ , and of similar magnitude for the accelerations. We thus imposed a-priori standard errors of these magnitudes upon the 4 parameters, and allowed the program to solve for all six unknowns.

In order to iterate the solution, at each stage we replace the predicted coordinates of the satellite by the displaced coordinates as determined from the previous solution. So for example

$$x = x + v_x \Delta T + l \Delta Q + x \Delta r/r$$

and similarly for  $y$  and  $z$ . It was found that 4 or 5 iterations were usually sufficient, where outliers of magnitude greater than  $3 \times \text{rms}$  were removed at each stage.

A selection of some plots of observational residuals is given in Figure 2, where it is clear that all trends have been removed; these residuals are readily used to form normal points using the Herstromonceux algorithm.

As a final check that the track of residuals is indeed statistically flat, we have introduced a single-factor analysis of variance test on the residuals. This test checks for significant differences between the means of residuals grouped into normal point bins; any differences indicate that not all trends have been removed from the residuals, and a warning is given that normal points should not be formed until the cause of the problem is traced. It is anticipated that this test may prove useful for the detection of system calibration changes during a pass.



### **3. Conclusion.**

The scheme was found to be determinate for a wide range of satellites and pass durations and quality of predictions, and has been adopted at Herstmonceux. An earlier version of the software is also in use at several European SLR stations. The deduced values of time bias are used to good effect for improving subsequent predictions, and additionally the software has been used to generate time bias values from the quicklook observations from other SLR stations, as described by Wood and Gibbs (these proceedings).

### **4. References.**

Gaignebet, J. (Ed) 1985. Recommendation 84A, Normal Points, in *Proc. 5th Int. Workshop on Laser Ranging Instrumentation*. CERGA, France.

Schutz, B.E. (Ed) 1990, April *Satellite Laser Ranging Newsletter*, Center for Space Research, University of Texas at Austin, USA.

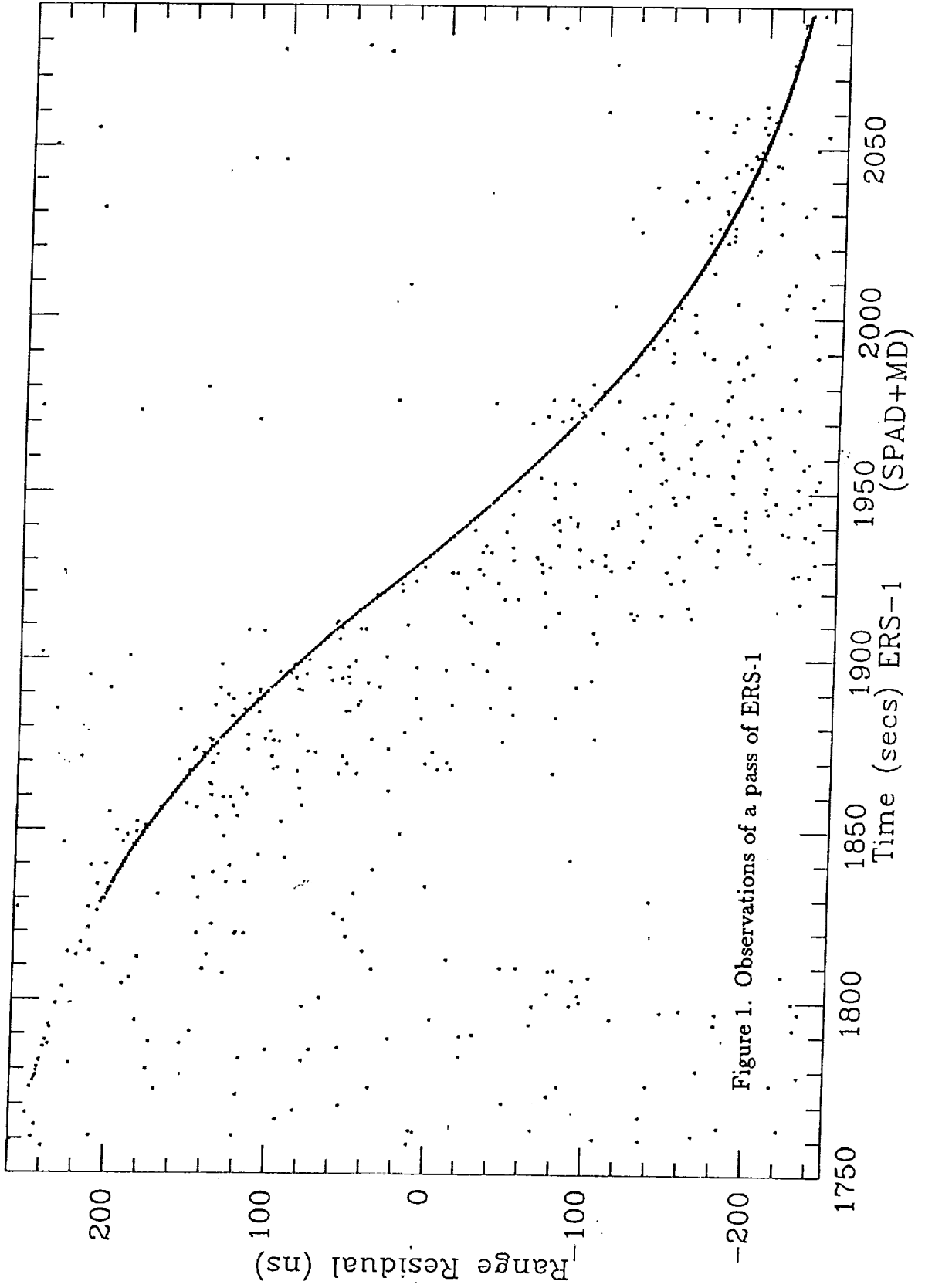


Figure 1. Observations of a pass of ERS-1

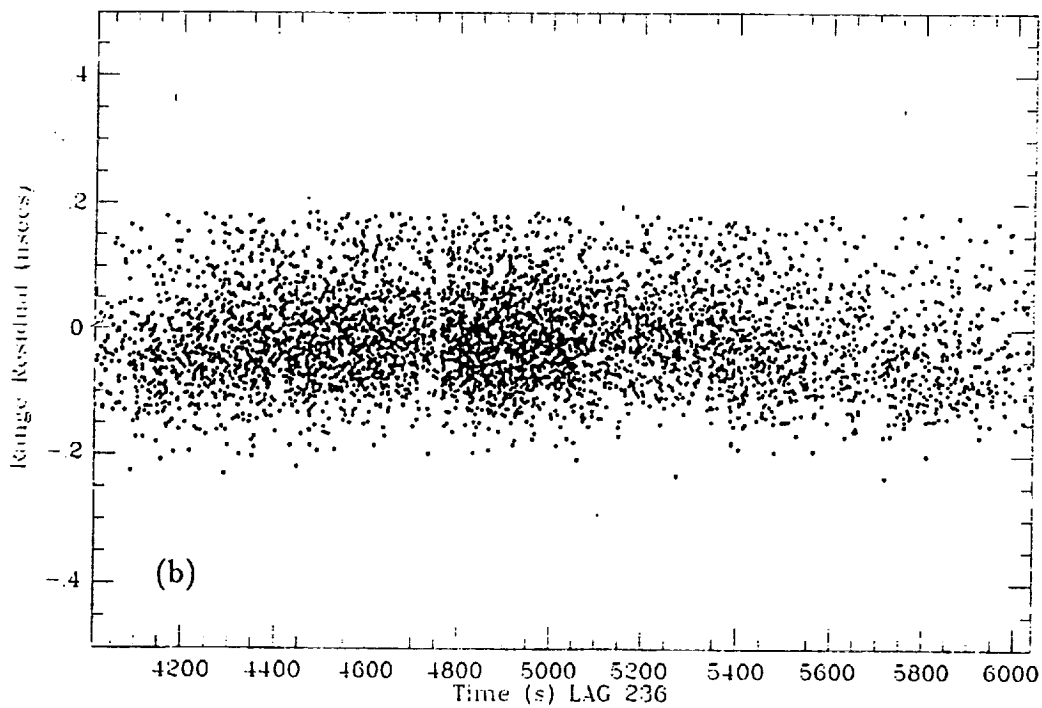
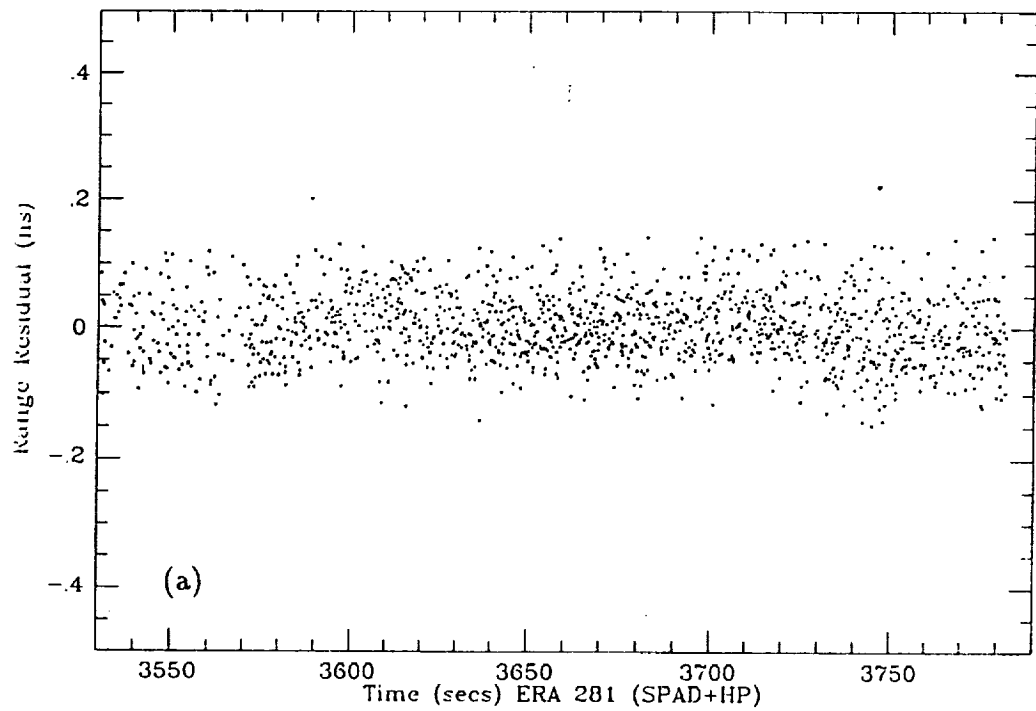


Figure 2. Range residuals from a pass of ERS-1 (a) and Lageos (b).

## Poisson Filtering of Laser Ranging Data

by

R. L. Ricklefs and P. J. Shelus  
McDonald Observatory, University of Texas, Austin, TX 78712

The filtering of data in a high noise, low signal strength environment is a situation encountered routinely in lunar laser ranging (LLR) and, to a lesser extent, in artificial satellite laser ranging (SLR). The use of Poisson statistics as one of the tools for filtering LLR data is described first in a historical context. The more recent application of this statistical technique to noisy SLR data is also described.

### Introduction

Routine LLR operations began at McDonald Observatory in August, 1969 as a part of the NASA Apollo Lunar Ranging Experiment (LURE), using the newly-commissioned 2.7-m astronomical telescope to range to the retro-reflector array placed upon the lunar surface by the Apollo 11 astronauts. During the next several years, additional arrays were left on the moon during the Apollo 14 and Apollo 15 missions, and by two Soviet unmanned soft landing vehicles. Routine LLR operations continued on the 2.7-m telescope until the mid-1980's when these operations were transferred to the dedicated 0.76-m aperture McDonald Laser Ranging Station (MLRS).

It is important to realize that the return signal strength ratio, neglecting all parameters except distance, for a near-Earth artificial satellite and the Moon is something like  $3 \times 10^{12}$ . Thus, it is more than a trillion times more difficult to range to the Moon than it is to range to, say, Ajisai. In the extremely low signal strength environment of LLR it was (and continues to be) necessary to operate largely at the single photon-electron level. However, this means that a very large number of "volunteer" photons from any number of background noise sources may trigger the detection electronics, even though very narrow spatial, spectral and temporal filters are routinely employed in the receive package. Since all incoming photons are indistinguishable from one another, identifying the valid returns from the moon has been a difficult task. From this experiment's inception, the reliance on statistical filtering methods, in addition to the physical ones, had been always assumed.

The application of Poisson statistics to the LLR data filtering problem provided an effective tool for dealing with high-noise, low signal data. The technique has now been expanded and adapted to handle marginal SLR data as well and has proven to be especially effective when applied to data from single or low-multiple photo-electron systems during daylight passes and data from all stations when they are ranging more difficult targets like Etalon-1, Etalon-2, and MP-2. Figures 1 and 2 show samples of noisy data, displayed by MLRS onsite software, for which the Poisson technique is required.

### Background

Let us consider the mathematical concept of the Poisson distribution, which gives the probability that a certain integer number,  $k$ , of unit rate random events from a population,  $n$ , will occur in a given interval of time,  $x$ , within some total interval of time. The operative equation is:

$$P(k) = \frac{x^{[k]} e^{-x}}{[k]!}$$

where  $[k]$  is the largest integer less than  $k$ . For  $x$  large enough, this function has a bell shape comprised of many rectangular steps. Multiplying the computed probability by the number of bins in the entire sample time gives the number of bins which contain exactly  $k$  events.

In a descriptive sense, Poisson statistics states that if one has "n" observations of some independent variable defined over some range of "m" bins of uniform width, and if those observations are random, one can compute, in a statistical sense, how many of those bins will contain exactly  $k$  observations. For example, for some specific experiment of, say, 16 independent observations of some value, one might compute from the above equation that 3 of the bins will be empty, 4 of them will contain exactly 1 observation, 3 of them will contain exactly 2 observations, 2 of them will contain exactly 3 observations, and no bins will contain 4 or more observations. Then, if one looks at the actual histogram of measurements and finds that one of the bins contains 8 of the 16 observations, one might safely assume that those observations are indeed not from a random distribution and that something systematic has occurred. In the case of LLR or SLR observations, where the measurement is an (o-c) range residual, it is assumed that the bin (or bins) containing a statistical excess of observations are probably valid returns from the target or the result of some systematic effect in the ranging equipment. As another example, figure 3 represents the statistics from the lunar data in figure 1. The predictions indicate that there should be no bins with more than 21 points. One bins has 22 points, which is probably not significant, but there is another bin with 47 points, which is significant. That bin contains the lunar data.

This technique is routinely applied to the filtering of McDonald Observatory LLR data and is fully described in "Laser observations of the Moon: Identification and construction of normal points for 1969-1971 by Abbot, Shelus, Mulholland and Silverberg (Astron. J., Vol. 78, No. 8, pp 784-793, October, 1973).

### Current state of affairs

In the routine application of the Poisson technique to data filtering it must be noted that, in order to have the best possible chance of isolating signal from noise, one should use the narrowest bin width possible, keeping in mind at all times, of course, the quantity being measured. Narrow bins will maximize the signal to noise ratio since, in a narrow-bin environment, a relatively small number of noise photons will be found in any one bin. Further, it is absolutely required that the data be flattened before a histogram is formed, i.e., trends must be removed from the data as much as is possible, so that signal will not "spill over" into many adjacent bins and, again, be lost in the "noise". This problem has been addressed in a straightforward way in the current data screening implementation at the MLRS, as shown in figure 4. All bins are scanned sequentially through a predetermined range of slopes, the plan being that the signal will appear at a significant peak at a slope that matches the inherent slope of the data. This technique is especially important for LLR data when signal strength is low and for SLR data when orbits are not well known. Of course, in altering the slope of the data, one must take care to exclude, or compensate for, those bins which will be incomplete due to clipping. In its present implementation at the MLRS, the Poisson screening software also allows multiple segments of a pass, or a run, to be treated separately. This handles the natural change in residual slope over an extended observation session.

Although personnel at the MLRS are now applying the Poisson filtering technique for both lunar and artificial satellite data, the LLR and SLR screening systems are somewhat different. Both systems provide user interaction to allow the selection of the parameters of the Poisson fit, placement of the time bins, maximum and minimum slopes, and a maximum and minimum residual for data to be accepted as "real". For lunar data, we employ fairly strict limits on acceptable slopes and allowable residuals. Earth rotation and polar motion are major contributors to slope and residual for lunar data, so the earth orientation predictions are kept as fresh as possible. Further, there is considerable latitude in selecting time bins to reflect the observed clumping of MLRS LLR data. Ultimately, the Poisson filter is relied on to provide the LLR data compression, i.e., normal pointing, software with a set of acceptable data.

For the SLR case, the Poisson algorithms serve as a preliminary filter and suggest to the polynomial fitting algorithms in the normal pointing packages a set of data with which to start. The polynomial fit, in its job, can then return previously rejected data back into the fit or remove data suggested to it by the Poisson filter, if either of these tasks are warranted. Also, the polynomial fit, working on the entire pass, can pull in data that might be missed or misinterpreted when the Poisson filter was working on only shorter segments of a pass.

The independent time segments, into which an SLR pass is broken, allow the software to follow changes in slope during a pass and minimize the effect of anomalous distributions of data in short segments. We are examining the desirability of having several software checks that require the slopes and average O-C residuals to be smoothly varying over the pass. However, in the cases where there are breaks in the data and other unusual distributions, this may not be practical.

## Results

In the case of LLR data, the presently implemented Poisson filtering technique works well, especially with a bit of interactive help from the user, although, in marginal cases, it would be preferable to use all runs taken over a lunar pass to aid in the filtering. This particular extension is now being examined. As time permits we are also pursuing more elaborate filtering techniques such as jack-knifing and bootstrapping to see if they hold merit.

In the case of SLR, the technique has been used successfully at MLRS for about a year now. In that time our experience has been that the combination of the Poisson filter and the polynomial fit produces good results virtually all of the time. The marginal cases can usually be satisfactorily processed, after the fact, by altering some of the parameter of the Poisson fit or by eliminating from consideration extremely noisy parts of the pass. Of course, most of the anomalies usually occur with weak passes, especially Etalon-1, Etalon-2 and ERS-1. The Poisson filter algorithms are being upgraded so that each satellite uses a parameter set tailored to it. Tests indicate that this will allow successful batch processing of virtually all passes that previously required special handling. Also, an interactive tool similar to the Lunar Data Editor is being developed to help the observing crews to quickly recover passes that were improperly processed. The Laser Tracking Network operated by the Bendix Field Engineering Corporation will soon install the MLRS "batch" Poisson code into their processing software.

## **Conclusion**

The Poisson filtering technique has proven itself to be an extremely valuable tool for both LLR and SLR operations at the MLRS. This technique is being optimized for each ranging target, and in the future provision will be made for routine, near-real-time observing crew interaction with the filter. In addition, new filtering techniques such as jack-knifing and bootstrapping will be evaluated as to suitability for laser ranging data filtering.

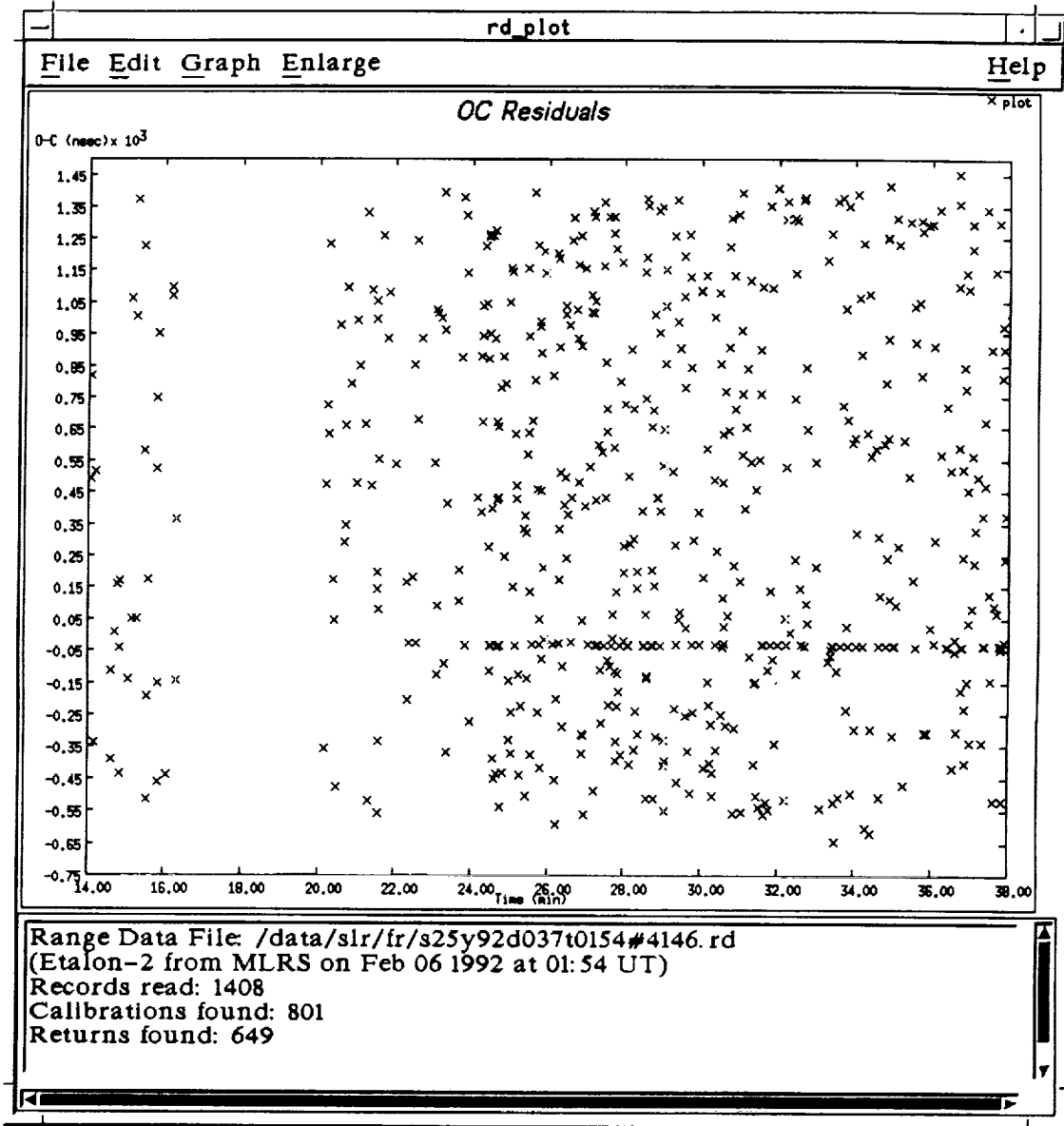


Figure 1 - Noisy Artificial Satellite Data



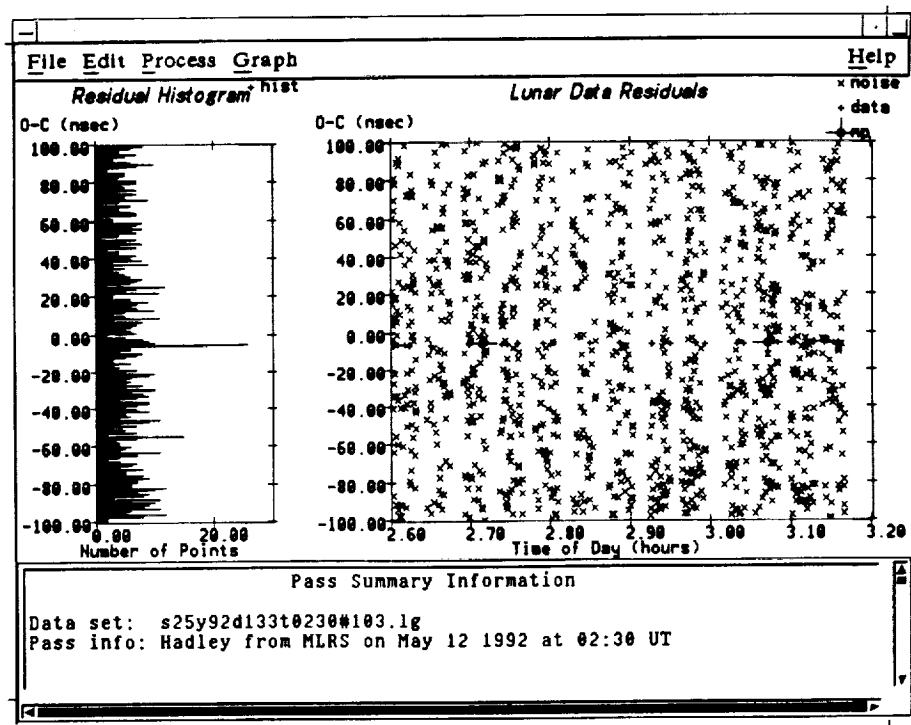


Figure 2 - Noisy Lunar Data

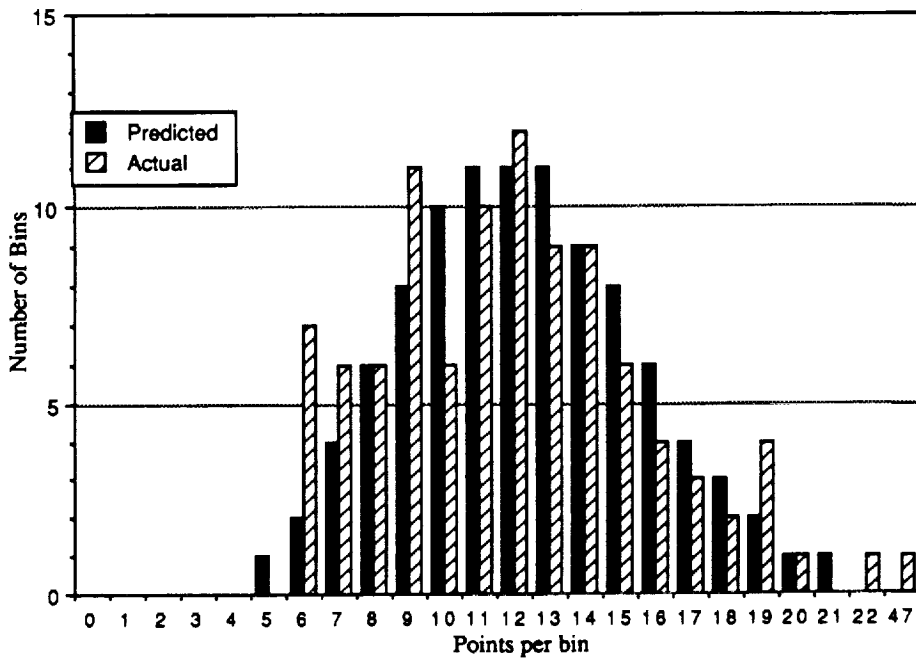


Figure 3 - Poisson Statistics for Sample Lunar Run

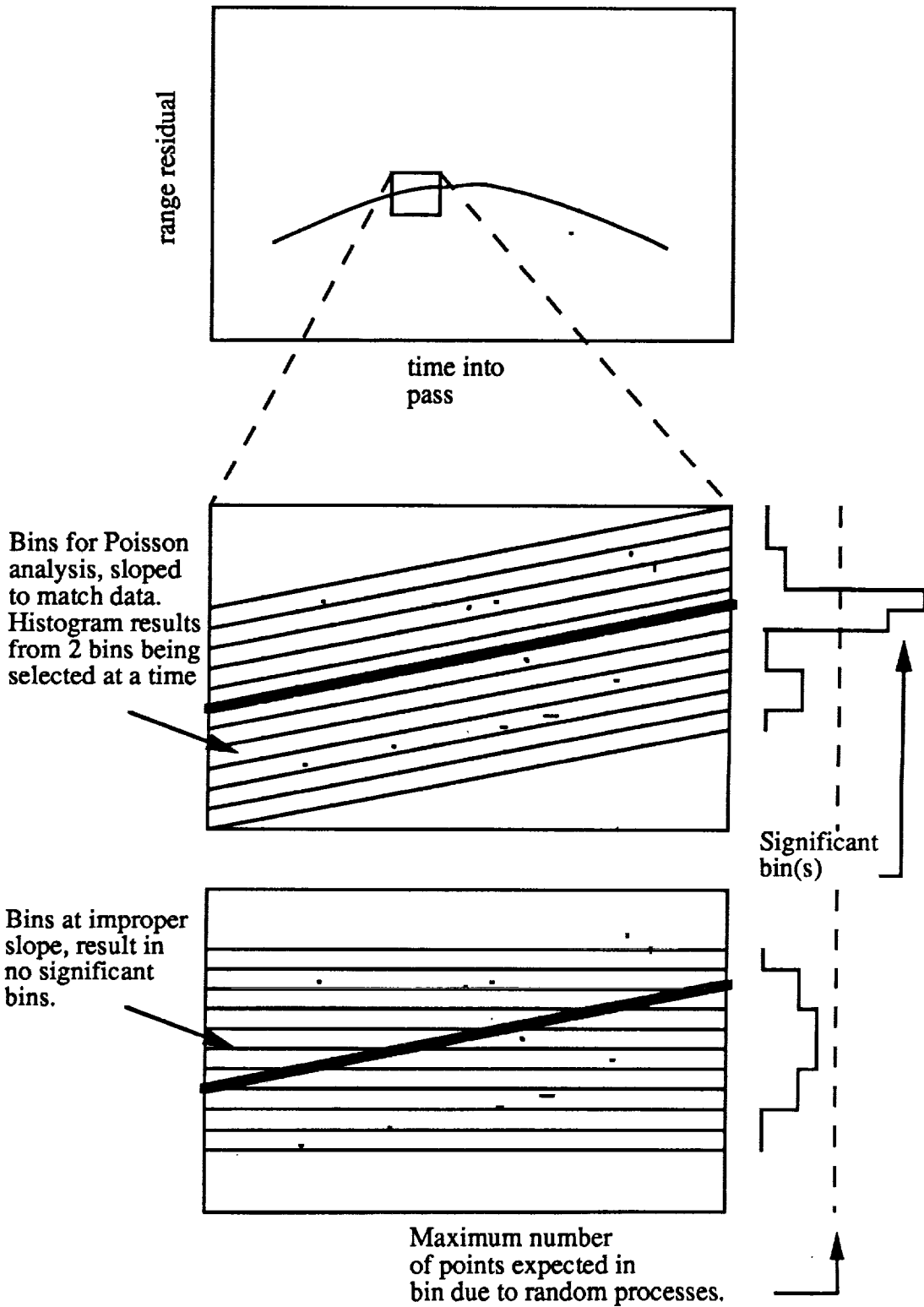


Figure 4 - Effect of Tilting Bins

Computer Networking at SLR Stations  
Antonín Novotný<sup>1</sup>  
Czech Technical University, Prague  
Czechoslovakia

Eighth International Workshop on Laser Ranging Instrumentation  
Annapolis, MD USA  
May 18-22, 1992

**Abstract**

There are existing several communication methods to deliver data from SLR station to the SLR data centre and back: telephonmodem, telex and computer networks. The SLR scientific community has been exploiting mainly INTERNET, BITNET/EARN and SPAN. 56 countries are connected to INTERNET and the number of nodes is exponentially growing. The computer networks mentioned above and others are connected through E-mail protocol.

The scientific progress of SLR requires to increase the communication speed and amount of the transmitted data. The TOPEX/POSEIDON test campaign required to deliver Quick Look data (1.7 kB/pass) from a SLR site to SLR data centre within 8 hours and Full Rate data (up to 500 kB/pass) within 24 hours.

We developed networking for remote SLR station in Helwan, Egypt. The reliable scheme for data delivery consists of: compression of MERIT2 format (up to 89%), encoding to ASCII file (files); e-mail sending from SLR station — e-mail receiving, decoding and decompression at the center.

We do propose to use ZIP method for compression/decompression and UUCODE method for ASCII encoding/decoding. This method will be useful for stations connected via telephonmodems or commercial networks.

The electronics delivery could solve the problem of the too late receiving of the FR data by SLR data center.

---

<sup>1</sup>e-mail: TJEAN@CSEARN.bitnet  
TJEAN@earn.cvut.cs

## The Name of the Game

The computer network backbone has spread all over the world.

Nowadays we may claim three axioms on network data exchange:

**Axiom 1.** *All non-local networks are connected to InterNet.*

**Axiom 2.** *All non-local networks have common protocol — mail protocol.*

**Axiom 3.** *The longer file is transferred, the longer it takes a byte to get through the network.*

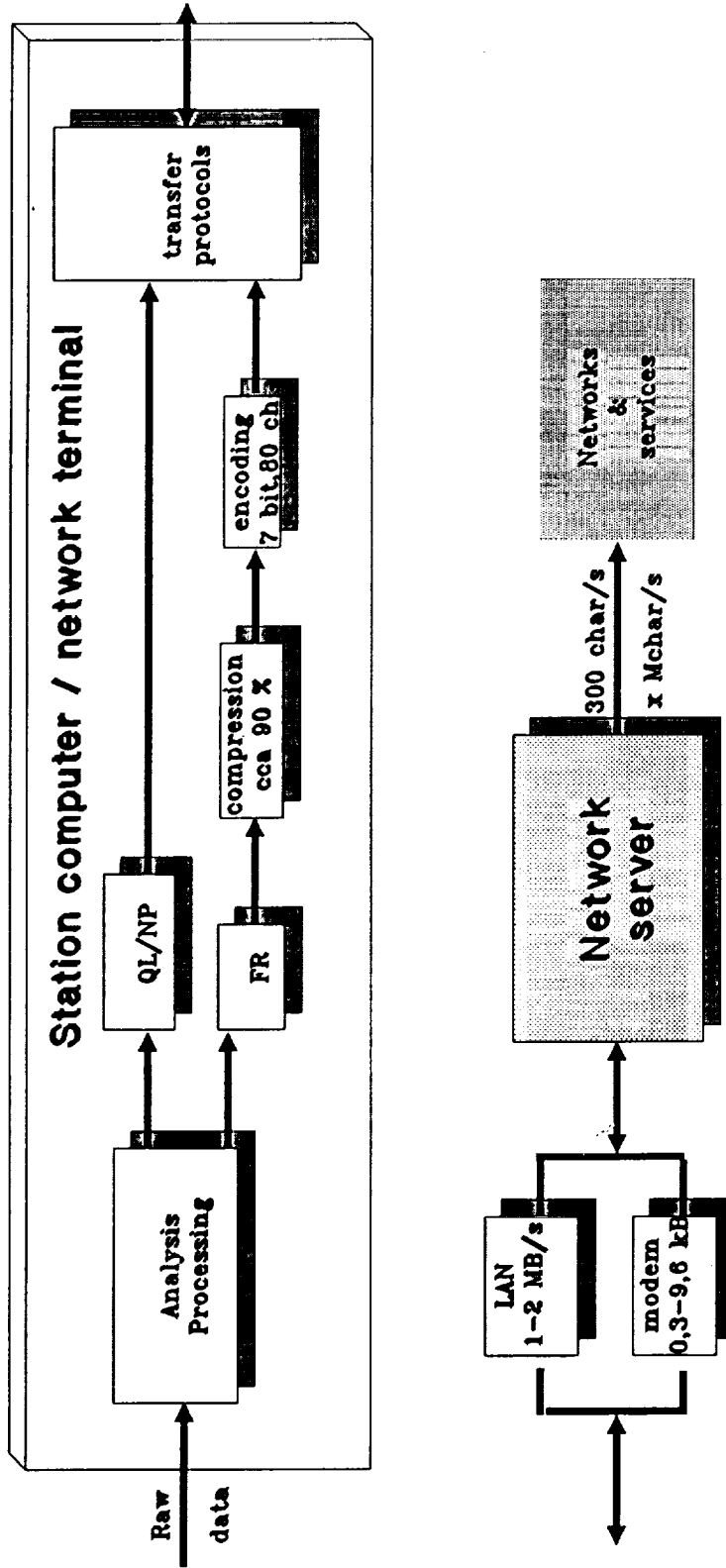
## Networking within the SLR Community

The most commonly used non-commercial networks are BITNet, InterNet, SPAN, UUCP. All are used on the satellite laser ranging facilities over the World.

The CSTG SLR Subcommittee Meeting in Pasadena, CA USA, March 12, 1992 agreed that, "InterNet will be implemented to all of the SLR and other DOSE related stations. This includes the stations in Russia and some of the other Commonwealth states that participate in the global network."

We will propose the new computer network standard for data handling between SLR data center and SLR stations. The following two figures schematically show one of the possible configurations.

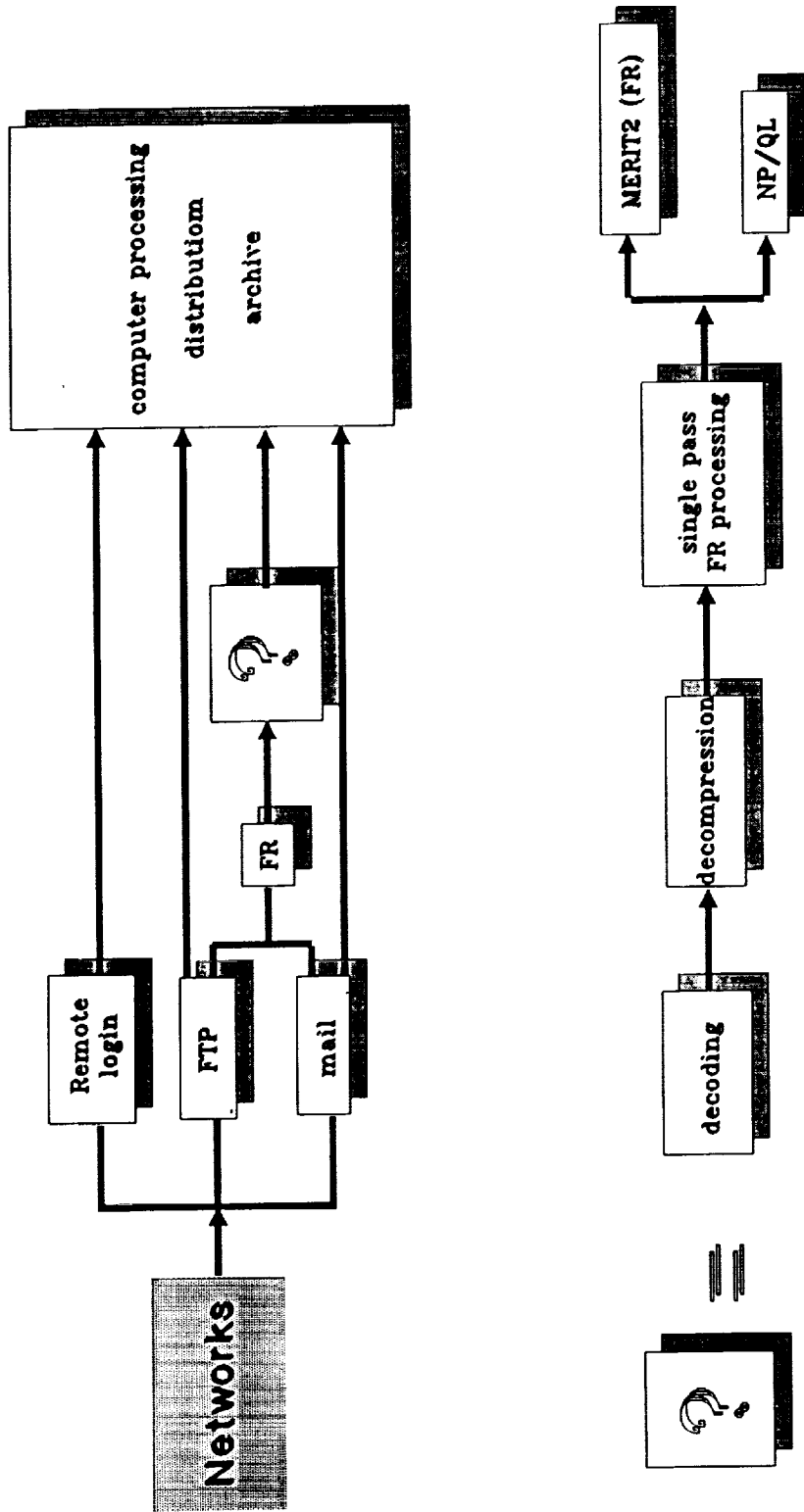
# Results handling at SLR stations



**Remark:** NP/QL data are redundant.

# Results handling at data center

NASA/BENDIX, Eurolas/DGFI



# Networks Data Exchange

## Mail at other networks

From the other networks, the files are sent to InterNet (and back) as a mail without any difficulties. The possibility of FTP (*File Transfer Protocol*) is strongly reduced to the use of mail servers.

### Selection of Large networks <sup>2</sup>

applelink	Apple Computer, Inc.'s in-house network
bitnet/earn	international academic network
bix	Byte Information eXchange: Byte magazine's commercial BBS
bmug	Berkeley Macintosh Users Group
compuserve	commercial time-sharing service
connect	Connect Professional Information Network
envoy	Envoy-100 (Canadian commercial mail service)
fax	Facsimile document transmission
fidonet	PC-based BBS network
geonet	GeoNet Mailbox Systems (commercial)
ieee-compmail	A DIALCOM system supporting IEEE users
internet	the Internet
mci	MCI's commercial electronic mail service
mfenet	Magnetic Fusion Energy Network
nasamail	NASA internal electronic mail
peacenet	non-profit mail service
sinet	Schlumberger Information NETwork
span	Space Physics Analysis Network
sprintmail	Sprint's commercial mail service
thenet	Texas Higher Education Network
usdamail	A DIALCOM system for USDA researchers

The more detailed information on mail network-to-network access see<sup>2</sup>.

## InterNet data transfer protocols

**FTP:** (*File Transfer Protocol*) Allows a user to connect to host computer and with reduced set of commands get and/or put files. FTP is essentially inaccessible from other nets. Getting files from FTP sites may be provided by mail servers (they retrieve the file and send it as a mail). Putting files by mail servers isn't supported. FTP is unfortunately slow (approx. 500 bytes/second, for longer files 200 bytes/second), the transfer rate depends on traffic in the network. The terminal must stay on-line while putting/receiving.

**Mail:** A convenient way for sending a file. A user has no possibility to receive files via mail (in sense that somebody must send the file, it can't send itself).

<sup>2</sup>© 1990 John J. Chew, available as EMAILGUI.ZIP at SIMTEL and TRICKLE archives

The transfer rate is a bit slower, but it does not keep local terminal busy as FTP does. Files longer than 50000 bytes are regarded as "huge" and sent only when the network is free.

Mail is essentially 7-bit protocol, 80 characters per line. Formatted or binary data can be converted to fit.

**TelNet:** Allows a remote login. Usefull for remote user access to any computer on the InterNet. Unusable for sending/retrieving files. User has to know remote computer's operating system.

Unfortunately, lots of SLR stations are not connected to InterNet and won't be connected soon. What's more, most stations have to use modems to connect to networks (which naturally slows down the transmission). That's why we should figure out how to send shorter files and how to send them from other networks.

## What Kind of Data Is Exchanged?

### 1. From SLR center to SLR stations

- Prediction (IRV or SAO)  $\approx$  5 kB
- Whole year IRV - Lageos  $\approx$  100 kB
- Comments on operation  $\approx$  2 kB
- Bendix QL analysis  $\approx$  1 kB
- Reports  $<$  25 kB

Suggestion: I would suggest the center to deliver these files to SLR stations as a regular mail to an automatic list of addressees. FTP makes the server at SLR center very busy while everybody is trying to receive the files. Due to the network software, when the network breaks down, it takes the biggest care of mail — it is almost always delivered. The FTP data might be easily lost or corrupted during breakdown. The non-InterNeters have to use mail-servers (for example BITFTP@PUCC) that may become very busy.

### 2. From SLR stations to SLR center

- Comments on operation  $\approx$  2 kB
- QL or NP data  $\approx$  2 kB/pass
- FR data MERIT2 format  
130 chars/line, 1 line/point  $\Rightarrow$  huge file  
up to 500 kB/pass  
This file is almost undeliverable via mail — it has more than 80 chars/line and



it has more than 50 kB. The Rules of a Network User say that user should never overload the network. In fact this file should never appear in mail! (And it might take several days/weeks to get through the networks.)

- **or** FR data compressed MERIT2 format and UUENCODEd — (compression 89%)  
This way of transmitting FR data solves almost all of the problems mentioned above.

## General Overview of Compression Techniques

- The good compression program must be easy to use, commonly used on different OS, must provide fast algorithm and high compression ratio
- Possible techniques:
  - ZOO:** Not very common, not very high ratio; source code available
  - LHA:** Not very common; very high ratio
  - TAR.Z:** Causes problems on non-UNIX OS, not very easy to use (on MSDOS), not very high ratio; very common on UNIX (supported by VAX/VMS)
  - ARC:** Out-of-date, slower than PKZIP; very common on many OS
  - ARJ:** New, not free for institutional use; very fast, the highest compression ratio, useful switches, starting to be used on lots of BBS's
  - PKZIP:** *Recommended*; very fast, good compression ratio, commonly used on most OS, sources available

## Encoding & Decoding

General rules for e-mail transmission:

- Convert 8-bit file and/or formatted file into 7-bit 80 chars/line file
- Split huge files (< 50 kB)
- Standard ENCODE/DECODE (UU & XX) programs are available for all network mainframes

Very comfortable shareware UUXFER program (with C sources) is available from D.M.Read (readm @ dopey.cc.utexas.edu)

### Features of UUXFER:

- Encoding UU, XX, using external table
- Decoding UU, XX (automatically detected)
- Optional splitting of huge files to user-defined size
- Merge file options
- Interactive/command-line commands
- User friendly
- Supports most of mainframes

## Conclusion

According to the Monthly Report on ERS-1 FR Laser Tracking Data Preprocessing, DGFI/D-PAF October 1991 (issued April 1992), it took up to three and half a month to deliver FR data from Simosato, Japan to the SLR Center (on the magnetic tape), and it took five (!! ) months to deliver data from Maidanak, CIC on floppy disks!!! This MUST BE CHANGED.

The electronic delivery via computer networks is the effective method to avoid the late delivery results from SLR sites..

### A. Requirements

- All SLR stations can access computer network
- Accepted standard for compression and/or coding
- Files have standard names for automatic processing at data center
- Sufficient operating hours of the involved networks including holidays
- Defined deadline time schedule for FR data delivery (in case QL, NP data would be sent by spare channel)

### B. Goals of computer networking at SLR world network

- NP/QL/FR data available for processing at SLR centers within less than 24 hours (hopefully)
- FR data would be transmitted instead of redundant NP and/or QL data
- Increased effectiveness when using data (delivered reliably and in time)
- Much cheaper data exchange

## Appendix

Network data exchange of huge data files was successfully tested from Helwan and from Prague during spring 1992

- Helwan — BITNET/EARN
- Prague — BITNET/EARN  
InterNet (the same mainframe)
- München — InterNet

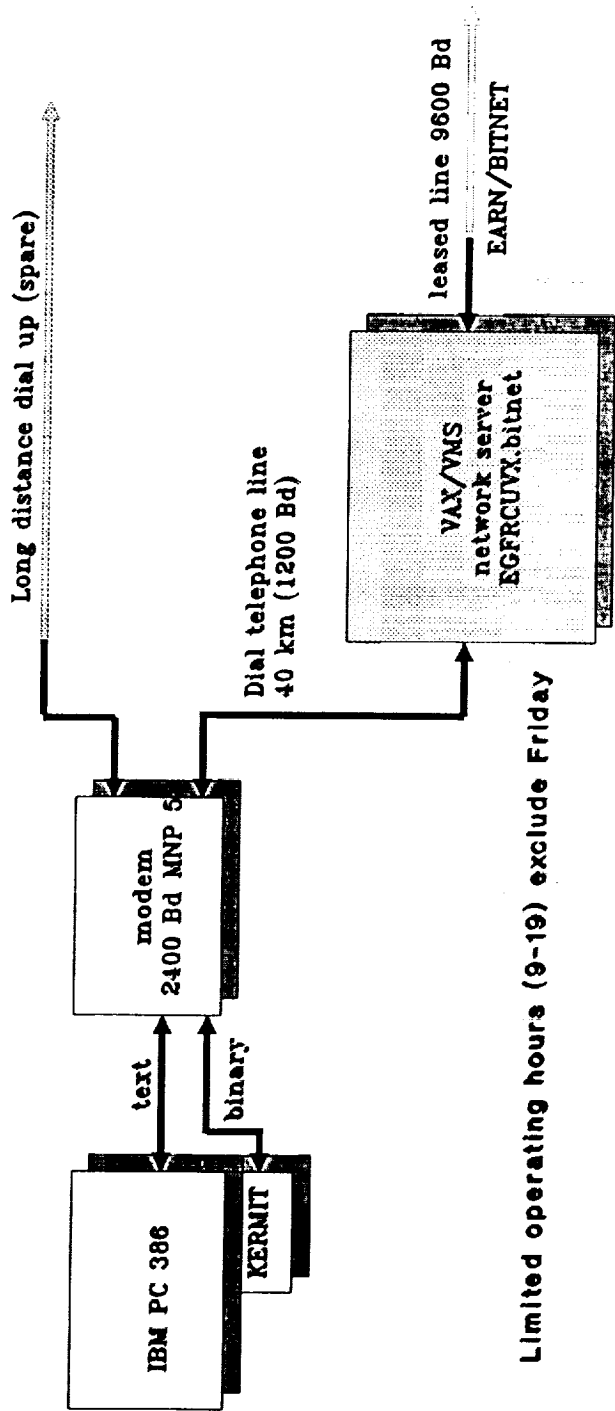
The Prague IBM mainframe was used as data center emulator

1. Helwan — compression, encoding
2. Helwan-Cairo VAX — by KERMIT ( $\approx 30$  B/s)
3. Cairo-Prague — BITNET (file transfer)  
BITNET-InterNet (mail)
4. Prague — decoding, decompression
5. Prague-München — FTP huge file transfer ( $\approx 100-700$  B/s)

All FR data from Helwan were delivered to Euro1as/DGFI by e-mail/FTP.

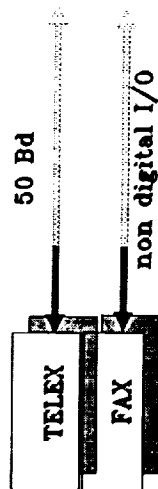
The communication facilities at SLR Helwan are described on the Figure.  
Remark: After the workshop, the problem was discussed with Dr. W. Seemüller. The Euro1as Data Center is ready to accept FR data as e-mail (compressed using PKZIP, encoded using UUENCODE/XXENCODE). I expect that all FR data from Helwan SLR will be delivered to EDC compressed and by e-mail from BITNet network.

# Communication facilities SLR Helwan



Limited operating hours (9-19) exclude Friday

## Spare:



# Upgrading NASA/DOSE Laser Ranging System Control Computers

by  
Randall L. Ricklefs  
McDonald Observatory, University of Texas, Austin, Texas 78712

Jack Cheek  
Hughes-STX, Lanham, MD 20706

Paul J. Seery, Kenneth Emenheiser, William P. Hanrahan  
Bendix Field Engineering Corp., Seabrook, MD 20706

Jan F. McGarry  
NASA Goddard Space Flight Center, Greenbelt, MD 20771,

Laser ranging systems now managed by the NASA Dynamics of the Solid Earth (DOSE) and operated by the Bendix Field Engineering Corporation, the University of Hawaii, and the University of Texas, have produced a wealth of inter-disciplinary scientific data over the last three decades. Despite upgrades to the most of the ranging station subsystems, the control computers remain a mix of 1970s-vintage minicomputers. These encompass a wide range of vendors, operating systems, and languages, making hardware and software support increasingly difficult. Current technology allows replacement of controller computers at a relatively low cost while maintaining excellent processing power and a friendly operating environment. The new controller systems are now being designed using IBM-PC-compatible 80486-based microcomputers, a real-time Unix operating system (LynxOS), and X-windows/Motif graphical user interface. Along with this, a flexible hardware design using CAMAC, GP-IB, and serial interfaces has been chosen. This design supports minimizing short and long term costs by relying on proven standards for both hardware and software components. Currently, the project is in the design and prototyping stage with the first systems targeted for production in mid-1993.

## Introduction

In the more than two decades of laser ranging, the observational accuracy of the NASA-funded laser stations has dropped from tens of centimeters to a centimeter or better. To achieve this, most parts of the ranging system have been upgraded a number of times. It has long been recognized that the computer subsystems are antiquated and unable to keep up with the requirements for ever-more-precise range measurements and an ever-growing list of targets. In the last year, a plan of action has been formulated to upgrade these systems in such a way as to minimize both short and long term cost by making extensive use of standard hardware and system software. The stations involved are the DOSE-operated GSFC 1.2m telescope, the Bendix Field Engineering Corporation-operated MOBLAS 4-8 and TLRS 2-4, the University of Hawaii-operated HOLLAS station, and the University of Texas-operated MLRS

## History

The controller computers on the DOSE network laser stations are late-1970s minicomputers produced by vendors such as Modcomp, Data General, and DEC. While they were real workhorses in their day, they are now eclipsed by faster, more expandable microcomputers an order of magnitude less expensive. Much of the code on these machines is written in archaic versions of FORTRAN which fail to meet even the FORTRAN 66 standards. A great deal of code is also written in the native assembly language of these machines. Many approximation and shortcuts were required to fit complex algorithms into these low-capacity computers. In some cases the operating systems are 'homebrew', while in other cases extensive changes have been made to no-longer-supported proprietary operating systems. If key personnel were to leave these organizations, the computer systems would be virtually unsupportable.

In addressing these issues, the CDP SLR Computer Committee decided in 1988 to off-load the data formatting, communications, and prediction functions of the existing controlling computers to dedicated Hewlett-Packard Unix workstations. These workstations were to also take on the tasks of data filtering and normalpointing. It was recognized at that time that replacing the controllers was a necessary task, but was too complex for the timetable necessary to support the burgeoning list of satellite targets. Figure 1 is a schematic of the current dual-computer system at the stations, with a serial line linking the computers. Since the process of implementing the new computers in the network laser stations is nearly complete, work has begun on the task of replacing the controller computers, a task made easier by the off-loading of many tasks to the workstations.

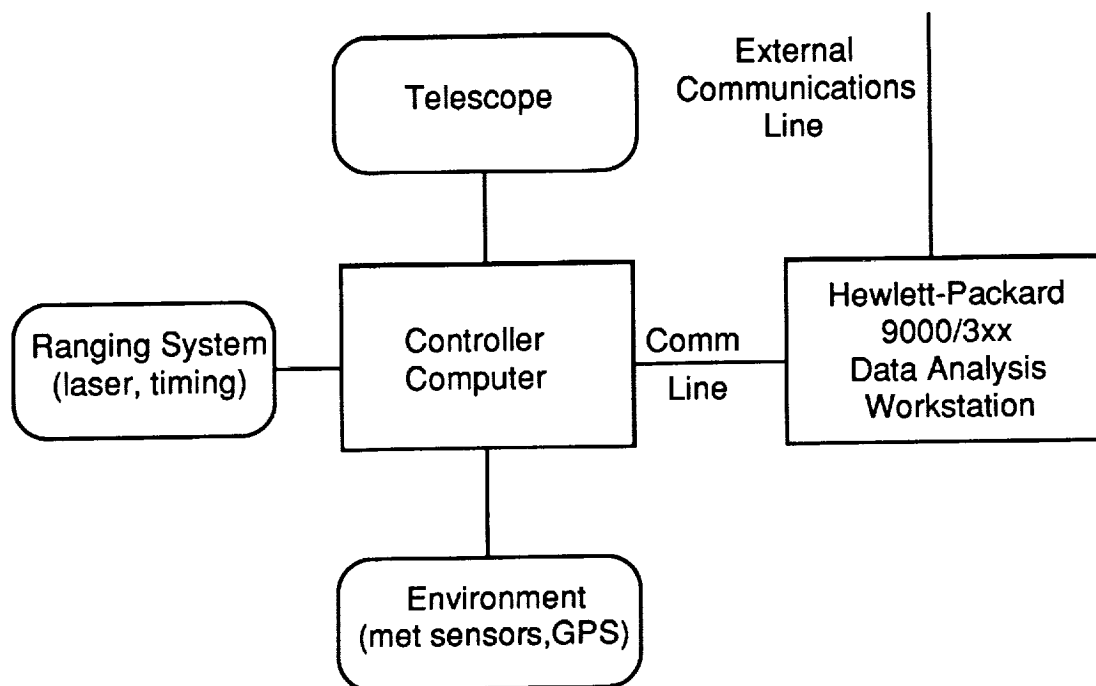


Figure 1: On-site Computer Configuration

## Hardware Environment

The new controller system must accommodate many of the vagaries of 7 or so laser systems' designs and philosophies and must be flexible enough to permit expansion of these systems in various ways. For instance, most of the Bendix-operated systems and the University of Hawaii system fire their lasers at 5 or 8 Hz, use external pre- and post-calibrations, and use Hewlett-Packard 5370 counters as time interval units. MLRS on the other hand, fires at 10 Hz, uses internal calibrations and uses a TD811 time digitizer as the finest part of its 3-tiered epoch timing system. The MOB LAS and transportable systems are limited to satellites up to the orbits of the Etalons. The GSFC 1.2m research system accommodates many experimenters, and ranges to aircraft as well as to satellites. MLRS ranges all currently targeted CDP satellites as well as MP-2 (in geostationary orbit) and reflectors on the moon. Some systems use CAMAC interfaces, while others use a proprietary bus interface standard. Some incorporate GP-IB (IEEE-488), and most use serial ports for various devices.

To replace the current controller computers, a new computer must be identified that can talk with each of the existing interfaces and that is likely to be supportable for the foreseeable future. It must support one or more real-time operating systems, and must be fast enough to meet all near term needs. Proprietary architecture and all the danger that implies must be avoided. In addition, the new system must be inexpensive. The obvious choice is the ubiquitous IBM-PC-compatible microcomputer. Boards exist that interface the PC to almost any variety of hardware; the upgrade path to an even faster machine than the prototypical 80486 33 MHz system is expected to be virtually painless; it is relatively inexpensive; and there are a number of reasonable real-time operating systems available.

A prototype systems design was developed which includes an IBM-PC clone containing a 33 Mhz Intel 80486, 16 Mb of RAM, a 330 Mb SCSI hard disk drive, 3 1/2" and 5 1/4" floppy disk drives, a 16 bit ethernet card, high resolution (1024 x 768) video display and a 16" monitor. Interface cards for CAMAC, GP-IB, and a serial mux board were also included. To save cost and space, the preliminary configuration will have the PC use both the printer and erasable optical disk on the HP workstation across the ethernet network.

To standardize the system interfaces and to limit dependence on specific vendors, it was decided to use the CAMAC, IEEE-488 (GP-IB), and RS-232 serial interfaces rather than dedicating a bus slot to virtually each device in a ranging station. Along these lines, the MOB LAS systems' obsolete IACC interface will be replaced by CAMAC, thereby removing an important source of maintenance difficulties. The serial ports are probably the easiest of all of these interfaces to accommodate with the PCs; they will be used to bring in environmental sensor data.

## Operating System

Each laser system involved in this project has evolved along a different path dictated by different needs. One overarching need now, however, is to create as much commonality as possible and to program for a software environment that will still be viable in 10 years. There were several options available when the search was made for operating systems, including writing it ourselves. Several of the current stations run home-built operating systems. The difficulties with these have been that they are hard to write and maintain. These systems were written because existing operating systems at the time did not offer the combination of speed, performance, and code size that was necessary to make the most

effective use of the hardware in a real-time environment. With fast and (relatively) inexpensive hardware, there are no such needs today.

In the search for an operating system, we considered DOS and DOS add-ons, various versions of Unix, and several proprietary operating systems, such as Digital Equipment Corporation's VMS and the Apple Macintosh Finder. The proprietary operating systems were rejected immediately, due to our need for vendor-independence. DOS and the Digital Research clone DR-DOS are neither multitasking, multiuser, nor realtime. DOS is also targeted to Intel 80x86 microprocessors, violating our requirement for vendor independence. Although products such as Microsoft Windows and DeskView offer some degree of multitasking, they do not claim to be either pre-emptive or real-time.

Unix was chosen because it has become a commonly available operating system with a rich software development environment. It does provide multi-user and multi-tasking capabilities and is available on many types of processors. Although there are several 'flavors' of Unix in the marketplace, the trend towards standards compliance allows well written programs to be transferred among Unix systems. The Hewlett-Packard workstations already available at the network laser stations run in a Unix environment. Standard Unix is not a real-time operating system. However, there are Unix clones and derivatives which do support realtime, pre-emptive multi-tasking and are designed for realtime acquisition and control applications like laser ranging.

A number of Unix and Unix-like systems were considered. These include:

Coherent (Mark Williams)	QNX (Quantum Systems)
REAL/IX (Modcomp)	Unix / Xenix (SCO)
VRTX (RadiSys Corp)	VxWorks (Wind River Systems)

The above were eliminated due to one or more of the following reasons. The operating system

- requires proprietary hardware
- did not mention POSIX or real-time standards compliance
- lacks one or more of the required compilers (FORTRAN, C, or assembler)
- lacks network capabilities
- lacks graphics capabilities

The chosen operating system is LynxOS by Lynx Real-Time Systems, Inc. LynxOS is a Unix-clone (no AT&T code) which complies with the POSIX standard as well as IEEE 1003.4 and 1003.4a draft real-time standards. It also follows the 80386 binary file standards and runs on IBM-PC compatible computers. LynxOS is also available for Motorola 680x0 systems and is being ported to the SPARC engine. C compilers (including one by GNU) are supplied with LynxOS, while FORTRAN is available from a third party. TCP/IP, NFS, X windows and OSF Motif are also available from Lynx. It should be mentioned for completeness that soon after LynxOS was chosen, Venix (Venturcom) was discovered. It uses AT&T system V code modified for real-time applications and also run on IBM-PC compatibles. It appears to be a viable alternative choice for a real-time operating system.

## User Interface and Networks

Several requirements for the user interface were advanced during planning. These included the need for a user-friendly interface, more graphics and less text, remote monitoring and control, automation of many hardware settings and seamless integration



with the HP workstation. The emerging standard for network-based, vendor-independent graphical user interface is the X windows system. Since X windows specifies no policy or style, there is no consistency required of applications. For this reason the Open Systems Foundation developed the Motif graphical user interface (GUI) on top of X windows, which does have a particular "look and feel". Open Look, which is another GUI supported by AT&T and Sun, does not seem to be as widely available at this time. Using the constraints of the GUI, user friendly applications can be produced that have many of the features of the familiar Apple Macintosh and Microsoft Windows applications, such as menu bars, pop-up windows, and freedom from a command line interface. Also, since X windows is network based, one can use the on-site software from virtually anywhere in the world via a network connection. Much of the experience gained and code developed in implementing such an interface for the on-site Hewlett-Packard workstations for the NASA-funded stations will be of great value in constructing the controller system.

Connecting the controller computer and on-site data-reduction workstation via ethernet and TCP/IP opens a world of data and control-sharing possibilities. Data can be recorded on the controller's disk drive in a directory which is mounted on the workstation via NFS (Network File System). The workstation can then have instant access to the data in real time. Sockets, RPC (Remote Program Calls), and remsh (remote shell) can all server as tools for creating a seamless dual computer system.

## **Preliminary Design**

In addition to agreeing on prototype hardware and software platforms, the GSFC 1.2m telescope, Bendix, and the University of Texas groups have all acquired prototype systems. Work is proceeding on the design of the user interface and underlying functions. Device drivers for two critical pieces of equipment - the CAMAC and the timing board (used to provide the computer with 20 Hz interrupts from the station clock) - have been written. The monitor program, which runs at all times and maintains information such as time, weather, and telescope status, and the star calibration program will be the first software package to be implemented, as they fulfil needs common to all stations. Work is also proceeding on replacement of the MOBLAS IACC interface with CAMAC. The goal is to put the first three upgraded systems (GSFC 1.2m, MOBLAS 7, and MLRS) into production with the new controller in mid to late 1993.

A preliminary version of the user interface is shown in figure 2. This shows the common display of station parameters maintained by the monitor program such as date, time and telescope position. Also evident is the pull-down menu and display of graphs and parameters unique to the star calibration program.

## **Conclusion**

The overdue upgrade of NASA ranging station control computers is finally coming about and is making use of the latest technology to produce a flexible, extensible, and maintainable computer platform. The upgrade is based on standard hardware and software components to lessen vendor dependence and enhance software portability. The prototype computer system has been designed and acquired by the principals in this upgrade, who are in the midst of further software design and low level software implementation.

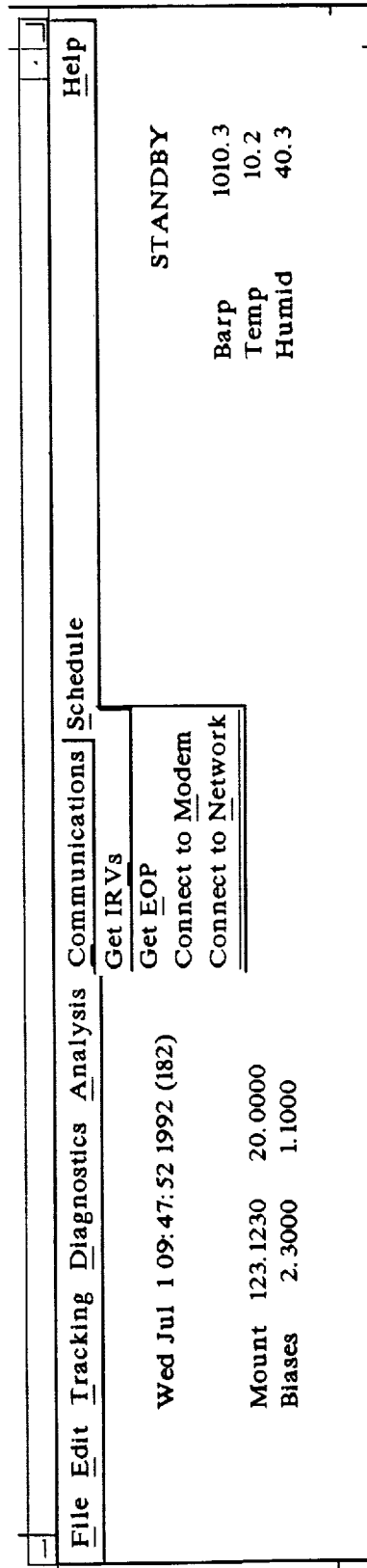
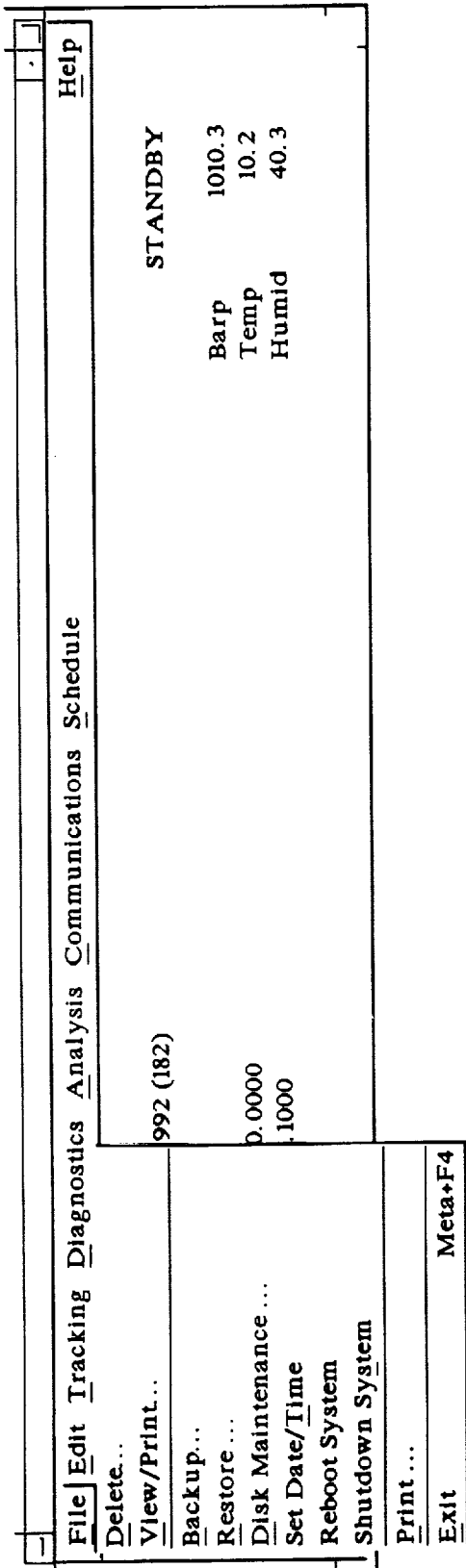


Figure 2 - Preliminary Monitor program user interface

## **HP UPGRADE OPERATIONAL STREAMLINING**

**D. Edge, K. Emenheiser, B. Hanarahan, D. McCollums, P. Seery**

**Allied-Signal Aerospace Company  
Seabrook, Maryland**

**R. Ricklefs**

**University of Texas  
Austin, Texas**

### **Abstract**

**New computer technology and resources must be successfully integrated into CDSLR station operations to manage new complex operational tracking requirements, support the on site production of new data products, support ongoing station performance improvements, and to support new station communication requirements.**

**The NASA CDSLR Network is in the process of upgrading station computer resources with HP UNIX workstations, designed to automate a wide range of operational station requirements. The primary HP upgrade objective was to relocate computer intensive data system tasks from the controller computer to a new advanced computer environment designed to meet the new data system requirements. The HP UNIX environment supports fully automated real time data communications, data management, data processing, and data quality control. Automated data compression procedures are used to improve the efficiency of station data communications. In addition, the UNIX environment supports a number of semi-automated technical and administrative operational station tasks. The x window user interface generates multiple simultaneous color graphics displays, providing direct operator visibility and control over a wide range of operational station functions.**

# HP UPGRADE OPERATIONAL STREAMLINING

The successful integration of new HP computer resources into the Crustal Dynamics Project (CDP) Satellite Laser Ranging (SLR) Network as part of the HP Upgrade Project has led to critically needed improvements in data system capability and significant gains in network operational efficiency. This paper provides a brief description of the HP Upgrade Project strategy and progress to date in streamlining station operations.

The HP Upgrade Project was initiated in 1987 to prepare the CDP SLR Network to meet the operational challenges presented by multi-satellite tracking operations in the 1990's. The technical approach for the HP Upgrade Project was based on the recommendations of the CDP Computer Panel, which recognized that new station requirements to support up to ten operational satellites and to produce on site normal points could not be supported by existing station computer resources. The existing computer resources recorded tracking data on floppy disk or magnetic tape and required manpower intensive operations to reload the data back into the computer to support station data processing activity. In addition, data processing operations and satellite tracking operations could not be performed at the same time. Therefore, data processing operations had to be scheduled around periods of operational tracking and were typically performed at the end of an operational shift. These problems delayed the production of data products and severely limited network tracking productivity. The basic HP Upgrade Project strategy was to integrate a second computer system into the existing station configuration to provide the required additional computer resources.

In 1988 the first HP computer systems were purchased, and development of HP Upgrade prototype systems started at the Goddard Space Flight Center (GSFC) and at the University of Texas. The development of a parallel prototype at the University of Texas was necessary to address the unique requirements of a lunar tracking station. HP UNIX software development projects were shared between GSFC and the University of Texas to reduce critical software development timelines and to maintain design consistency.

The Moblas 7 and MLRS HP prototype systems were successfully tested in 1990. In 1991, the HP Upgrade was deployed to the remaining network operational Moblas systems and development started on HP Upgrades for TLRS 3, TLRS 4, and Hollas. The TLRS 3, TLRS 4, and Hollas HP Upgrades are expected to be completed in 1992.

In order to reduce the load on critical station manpower and computer resources, the HP data system was designed to provide fully automated data communications and data processing during multi-satellite operations. Figure 1 presents a simplified diagram of HP data system functions. The functions associated with real time tracking operations are divided between the controller and HP computers. Other Non real time HP functions, which include general station operations and automated post tracking functions complete the automated HP Data System Product Cycle. Depending on the number of observations in the pass, the HP Data System was designed to produce the normal point data product 1 to 5 minutes after the operator has closed out the operational data set. The time

required to compress the normal point data set and transmit the data product to headquarters is less than 1 minute.

The HP Data System has built in flexibility which allows interleaving of multiple satellite and calibration sets. The code has been written to allow for many different combinations of hardware settings. This has been accomplished via the use of different levels of ranging activity. By changing levels within the software, the operator may determine which calibration sets (with possibly different hardware characteristics) go with which satellite sets. Up to five different levels may be selected. This feature makes it possible to quickly switch from one satellite to another and back again using calibration sets which may be unique for each satellite. Figure 2 is an example of a single shift of Moblas 4 support scheduling multiple satellite and calibration operations. Scheduled ERS-1, Ajisai, Lageos, Etalon 1, Etalon 2, and Starlette passes are labeled E1, AJ, L1, MT, NT, and ST respectively. Scheduled calibration tracking is labeled C1. The activity scheduled at the bottom is the sum of scheduled satellite and calibration activities. The station is continuously ranging satellites or the calibration target for over 5 hours during the shift. The scheduling of multi-satellite operations has significantly increased the operational productivity of operational laser stations. Additional information concerning the scheduling of multi-satellite tracking operations is presented in another Eight International Workshop on Laser Ranging Instrumentation paper "SATCOP Mission Planning Software Package".

Control of all processing and maintenance operations is provided by a mouse and/or keyboard driven, user friendly multi-level menu interface. These menu controlled operations include data archiving, tuned IRV prediction communications, data product statistics review, station communications, semi-automated daily tracking operations reports, and other general station data communications. The user interface is written in the 'C' programming language and uses the Motif/x windows style and flavor. The use of this industry standard ensures that the user interface is consistent with other operating systems (in addition to UNIX) and is also consistent with widely available off-the-shelf commercial software.

The design prototype for the second "processing" computer system was a UNIX based HP 360 workstation. Low cost upgrades have brought the design prototype up to the current CDP SLR network configuration described in Figure 3. The HP 380 computer configuration includes two 332 MB hard disks to improve efficiency by directing data operations to one disk and operating system functions to the other disk. A 650 MB optical disk is included to provide on line data archiving, a efficient backup media, and to support major software system upgrades. The 67 MB cartridge tape is used as a low cost media for generating weekly full rate mailing tapes. The HP Paintjet printer supports local hard copy requirements. The 19.2k baud modem supports a wide range of station communication requirements including data communications and software system updates. The 16 inch color supports the X-Window environment and is the primary user control interface device for the HP Data System.

The Moblas, MLRS, TLRS, and Hollas systems all have unique controller computer hardware and software environments. Real time control functions may also vary station to station (MLRS is a lunar station, for example). The HP Upgrade development strategy was to minimize the impact on real time controller functions, requiring only real time data communications to the HP "processing computer" and off load as many non real time functions as possible from the controller to the "processing computer". A simplified functional block diagram for TLRS 3/4 is presented in figure 4. The controller

(or tracking) computer performance in managing the real time computer interfaces was a key technical design problem for each station type.

Real time applications were developed in C in the HP UNIX environment to record and manage the flow of raw data measurements from the controller computer to the HP 380. Automated C and Fortran applications assemble, screen, and prepare the raw data measurements for automated data processing. Based on inputs from the system operator, automated data processing functions start as soon as the raw data set is complete.

The HP UNIX software environment, which includes FORTRAN and C applications, was selected to make maximum use of existing operational software, provide multi-vendor hardware portability, and to provide a robust industry x window user interface for station operations. The HP Upgrade Project software strategy was to develop real time applications in C and other data system applications in FORTRAN to make the best use of current operational software. The station user interface was developed in the HP UNIX x window environment to make the best use of the HP 380 workstation resources in controlling station operations.

In order to meet the new station normal point data system requirements and maintain data system integrity, operational data system software was rehosted from VAX/VMS Fortran to HP UNIX Fortran. The field data processing system was designed to use identical data processing algorithms and to perform the same basic data processing and data quality control functions as the operational headquarters system. These data processing functions include quality control of raw data measurements, calibration data processing, computation of satellite ranging corrections, analytical satellite data fitting, and satellite data compression to form normal points. The field data processing system was designed to produce the same operational quality control statistics and data products as the headquarters system. These data statistics and data products were carefully benchmarked against the operational headquarters data system before the HP Data System was declared operational. Some software system utilities used in the VAX/VMS environment had to be replaced with equivalent HP UNIX utilities during software rehosting.

The HP Data System Upgrade has been successfully operating at Moblas 4, Moblas 5, Moblas 7, and MLRS for over a year, producing on site normal points, generated within minutes of operational satellite tracking. Starting in April 1992, multi-satellite operations were successfully integrated into the HP Upgrade Data System, contributing to recent record data production by Moblas 4 and Moblas 8. Upgrades to the HP workstation CPU's have been successfully accomplished in the field without software system modifications and have enabled the HP Data System to accommodate massive increases in data volume associated with multi-satellite operations and two shift network support for TOPEX. Remote software system updates have been performed using modem communications, without impacting station operations. The automation of the Data System has helped free up critical station manpower resources needed to sustain nearly continuous tracking operations associated with multi-satellite support. The HP Upgrade is the first major step in streamlining CDP SLR operations. Strategic technical planning to replace the controller computer, providing necessary computer resources to automate other station functions, is in progress. In addition, direct computer network communications to CDP SLR network stations is expected to be established in the near future, providing advanced communication resources to automate remote software system management activities and global data communications.

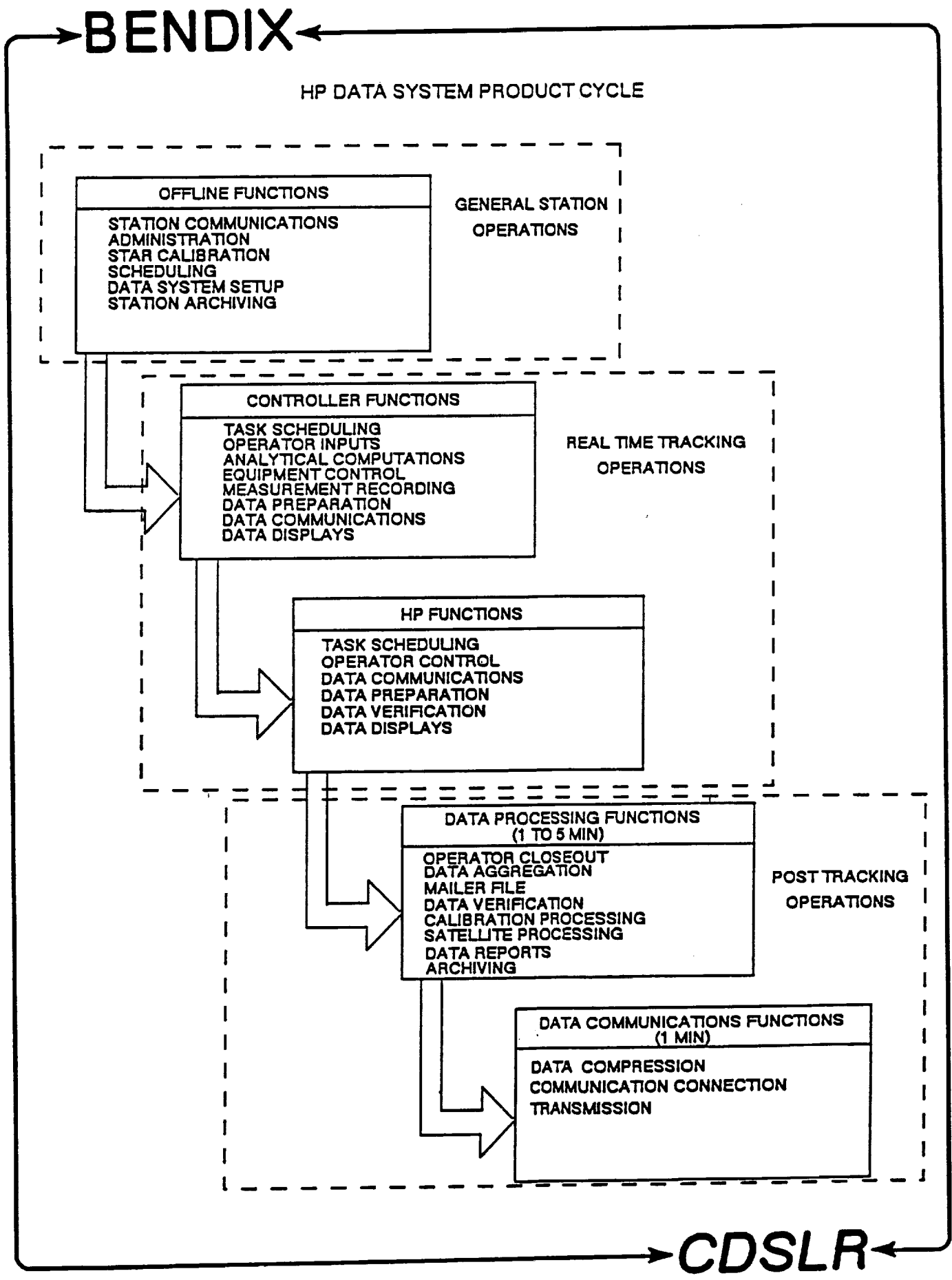
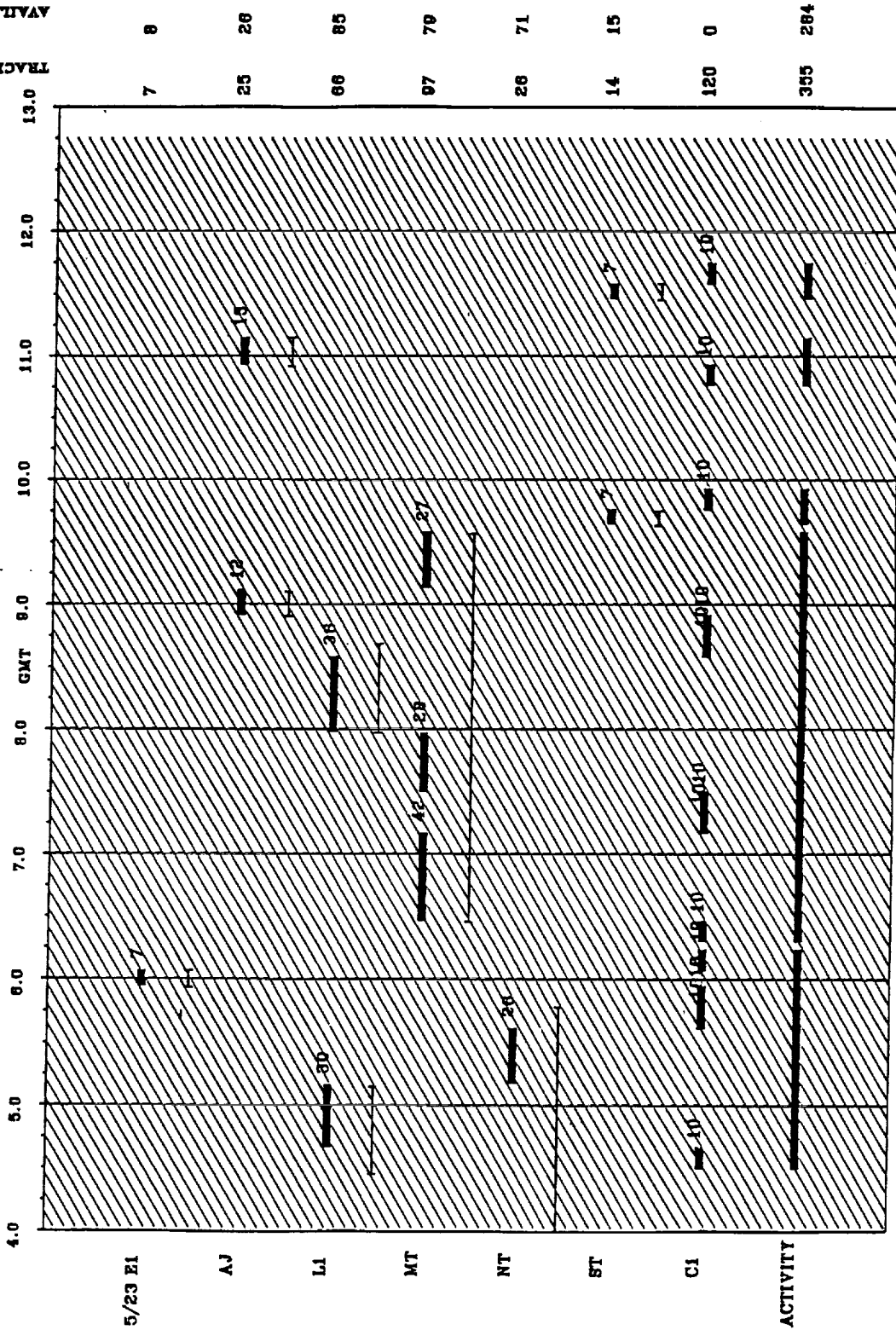


FIGURE 1

**BENDIX**

**SATELLITE VISIBILITY: MOBIL4 (711U)  
5/23/92 - 5/23/92 SHIFT NUMBER 1**

(MINUTES)  
TRACKING AVAILABLE



date created: 5/15/92  
 BFEC/CDSLRL DSO Bucey Conklin  
 THICK SOLID CURVE IS ACTUAL TRACKING.  
 ATTACHED THIN CURVE IS PRE/POST CAL TIMES.  
 NOTATION ON PASS IS MINUTES OF PASS TRACKED.  
 SINGLE THIN LINE IS ACTUAL VISIBLE PASS.  
 SHADED SECTION IS NIGHT.

**CDSLRL**

FIGURE 2



# TLRS 3 HP 380 COMPUTER SYSTEM

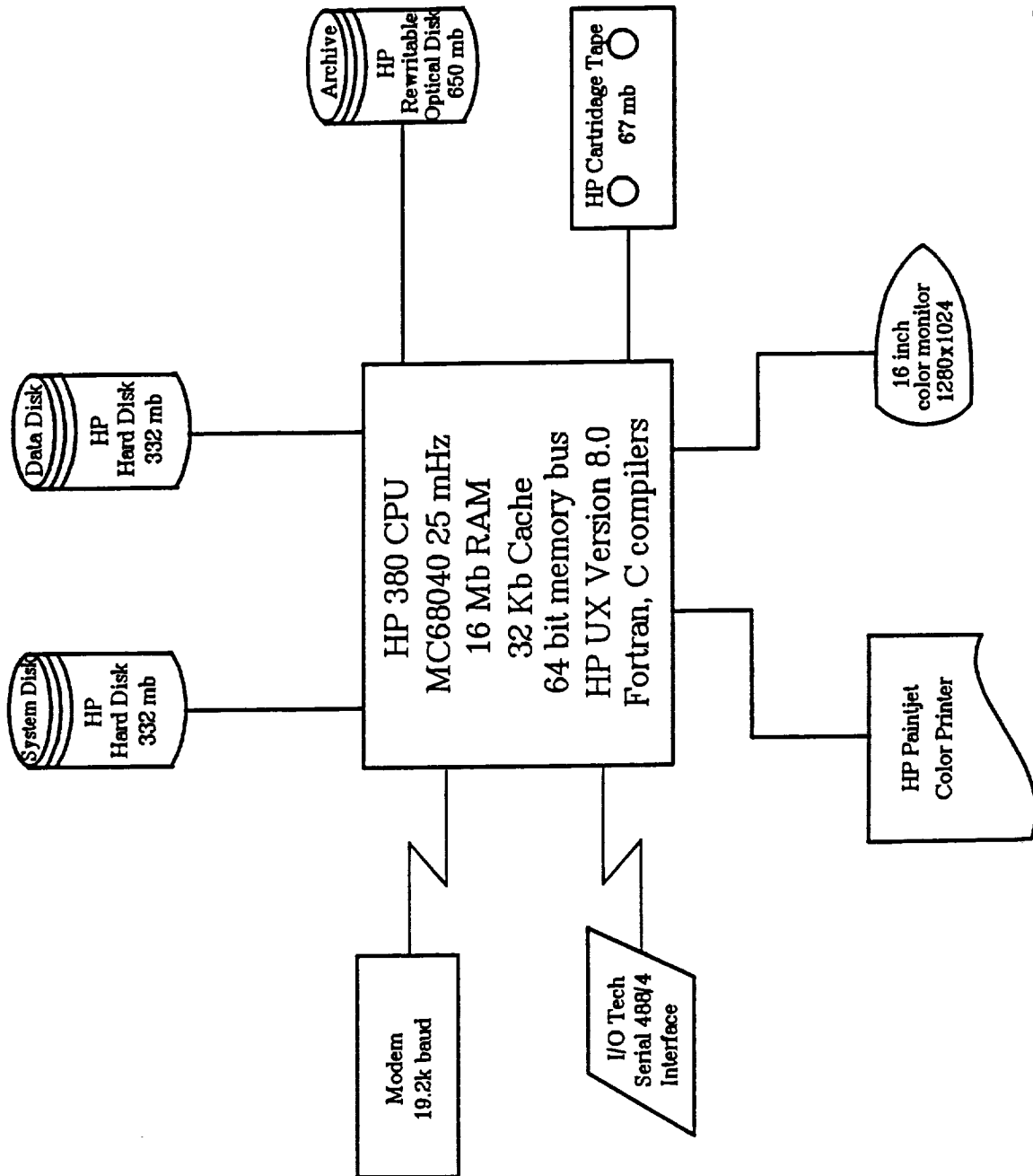


FIGURE 3

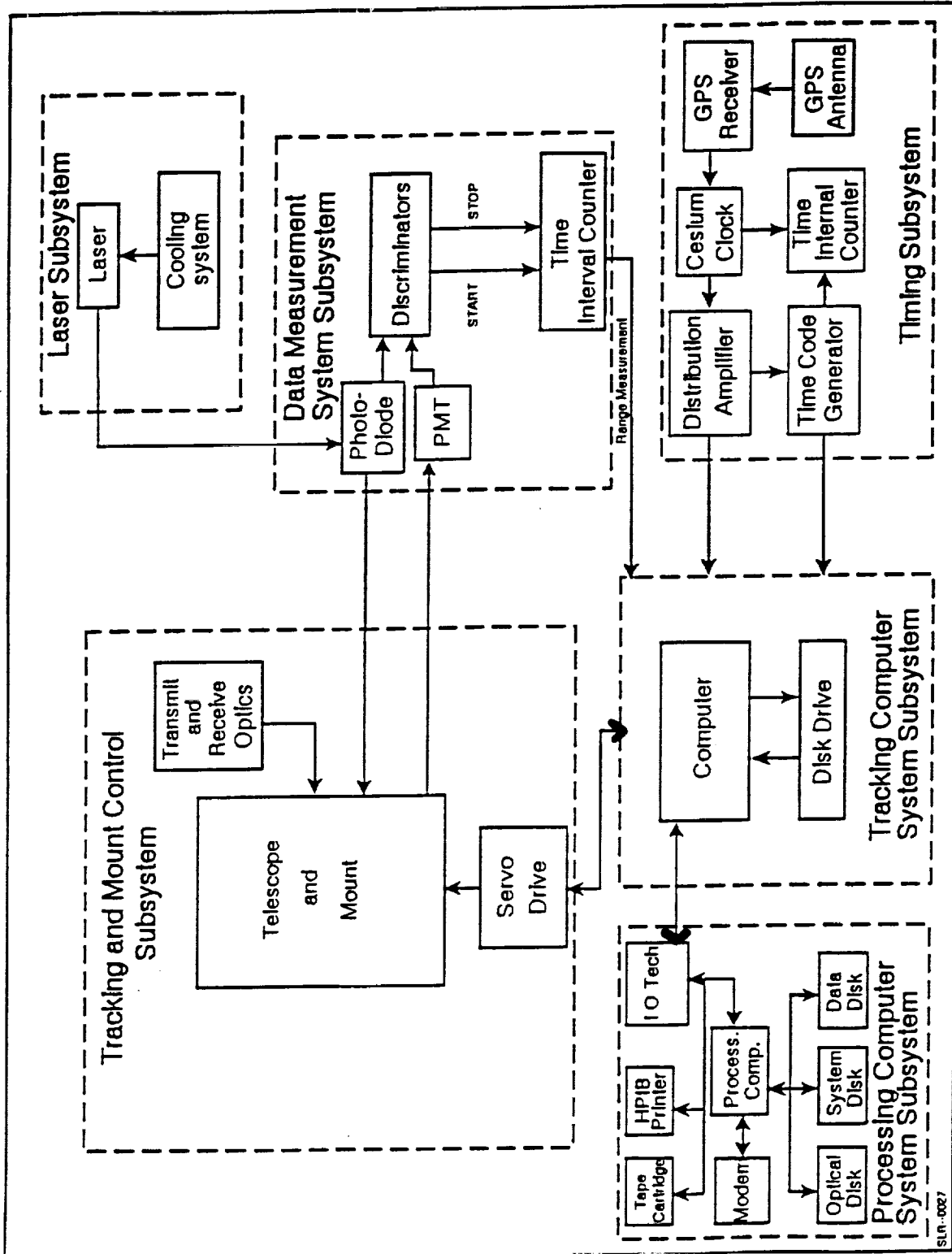


FIGURE 4

N94-15597

APPLICATION OF THE ROBUST ESTIMATE  
IN SLR DATA PREPROCESSING

T. Detong, Z. Zhongping, X. Huaguan  
Shanghai Observatory  
Academia Sinica

J. Peizhang  
Institute of Systems Science  
Academia Sinica

ABSTRACT

M-estimator, one kind of robust estimator, has been used in SLR data preprocessing. It has been shown that the M-estimator has 50% or more breakdown point.

# APPLICATION OF THE ROBUST ESTIMATE IN SLR DATA PREPROCESSING

Tan Detong, Zhang Zhongping, Xu Huaguan  
Shanghai Observatory  
Academia Sinica

Jia Peizhang  
Institute of Systems Science  
Academia Sinica

## INTRODUCTION

There are three purposes in preprocessing from a pass of raw satellite range measurements:

- a) Correcting system errors for raw SLR data and forming observational files;
- b) Fitting a smoothing function to the range residuals from the predicted orbit, rejecting noises and outliers then estimating accurate for this pass;
- c) Forming QL, FL and NP data files.

The second term is very important for data preprocess, because the smoothing function will have effect on quality of NP data.

The smoothing function we used is simply a polynomial in time. Generally, the least squares (LS) estimation is used to solve the parameters of polynomial. But, the LS estimation is not a robust estimation. Sometime, there are a large number of noises in raw SLR data, especially those passes are in daylight, the solution of the LS estimation will converge to false values.

In this paper, M-estimator, one kind of robust estimator has been used in SLR data preprocessing. It has been shown that the M-estimators has 50% or more breakdown point  $\varepsilon^*$ . The breakdown point means that, when the probability of noises  $\varepsilon$ , increases to  $\varepsilon^*$ , this method will fail.

## M-ESTIMATOR

The linear equation is written:

$$y_i = X_i^T \theta + e_i \quad (1)$$

where

$y_i$  are observations

$\theta$  is the vector of parameters to be estimated  
 $X_i$  is the vector of coefficients  
 $e_i$  are random errors.

The M-estimator, called Maximum Likelihood Type Estimator, is such an estimator which makes the following objective function minimum:

$$\sum_{i=1}^N F((y_i - X_i^T \hat{\theta})/\sigma) = \min. \quad (2)$$

$\hat{\theta}$  are values estimated for  $\theta$

$\sigma^2$  is variance

$F(\cdot)$  is an even function

Different objective functions have different M-estimator. In this paper we used Hampel estimator, here

$$F(r_i) = \begin{cases} \frac{1}{2} r_i^2 & |r_i| \leq \lambda_0 \sigma \\ \lambda_0 \sigma (|r_i| - \frac{1}{2} \lambda_0 \sigma) & \lambda_0 \sigma < |r_i| \leq \lambda_1 \sigma \\ \frac{\lambda_0}{\lambda_2 - \lambda_1} (\lambda_2 \sigma |r_i| - \frac{1}{2} r_i^2) & \lambda_1 \sigma < |r_i| \leq \lambda_2 \sigma \\ \frac{\lambda_1}{\lambda_2 - \lambda_1} \frac{\lambda_0}{2} \sigma^2 - \frac{1}{2} \lambda_0^2 \sigma^2 & |r_i| > \lambda_2 \sigma \\ \lambda_0 (\lambda_2 + \lambda_1 - \lambda_0) \sigma^2 / 2 & |r_i| > \lambda_2 \sigma \end{cases} \quad (3)$$

$$r_i = y_i - X_i^T \hat{\theta}$$

$$\lambda_0 = 3, \lambda_1 = 4, \lambda_2 = 6.$$

Equation (2) can be rewritten as:

$$\sum_{i=1}^N X_i \Psi((y_i - X_i^T \hat{\theta})/\sigma) = 0 \quad (4)$$

where

$$\Psi(\cdot) = F'(\cdot).$$

Then

$$\hat{\theta} = \left[ \sum_{i=1}^N X_i W_i X_i^T \right]^{-1} \left[ \sum_{i=1}^N X_i W_i y_i \right] \quad (5)$$

and

$$W_i = \Psi(r_i/\sigma) / (r_i/\sigma). \quad (6)$$

From (3) we have

$$W(r_i/\sigma) = \begin{cases} 1 & |r_i| \leq \lambda_0 \sigma \\ \lambda_0 \sigma / |r_i| & \lambda_0 \sigma < |r_i| \leq \lambda_1 \sigma \\ \lambda_0 (\lambda_2 \sigma - |r_i|) / (\lambda_2 - \lambda_1) |r_i| & \lambda_1 \sigma < |r_i| \leq \lambda_2 \sigma \\ 0 & |r_i| > \lambda_2 \sigma \end{cases} \quad (7)$$

and

$$\hat{\sigma}^2 = \frac{1}{N-p} \sum_{i=1}^N r_i^2 \quad (8)$$

p is number of the paramaters estimated.

When given the starting values  $\theta_0$  and  $\sigma_0$ , we can solve  $\hat{\theta}$  by (5), (6) and (7). The solution is then iterated between (5) and (8), until convergence of the object function.

$$|U^{j+1} - U^j| / U^j < 10^{-3}$$

here

$$U = \sum_{i=1}^N F\{(y_i - X_i^T \hat{\theta}) / \sigma\}$$

j is the times of the iteration.

## PROCEDURES

The predicted and observed ranges is  $R_c$  and  $R_o$  at each instant of observation T. After atmospheric correction, center of mass correction and delay calibration, we have the following range residual equation:

$$\begin{aligned} y_i &= \Delta R_i \\ &= a + b \dot{\rho}_i + e_i \end{aligned} \quad (9)$$

Where a, b are range bias and time bias.

$\dot{\rho}$  is the variability of range.

Reference show a method of caculation which have 50% breakdown point.

a) If total observation data points are N, which are divided into n subgroups equally and every subgroup includes four data points, as:

$$\begin{array}{cccc} y_1 & y_{n+1} & y_{2n+1} & y_{3n+1} \\ y_2 & y_{n+2} & y_{2n+2} & y_{3n+2} \\ \dots & \dots & \dots & \dots \end{array}$$

$$\begin{array}{cccc}
y_k & y_{n+k} & y_{2n+k} & y_{3n+k} \\
\dots\dots & & & \\
y_n & y_{n+n} & y_{2n+n} & y_{3n+n}
\end{array}$$

$$n=N/4.$$

When noise numbers in raw observation data are less than  $N/2$ , there must be a subgroup in which contains one noise point at most.

b) For the linear model as (9), we can find the linear estimated value of  $\hat{b}_k$  for any subgroup  $k$ :

$$\hat{b}_k = \sum_{i=1}^4 \beta_i y_i \tag{10}$$

If  $\hat{b}_k$  is no-bias, we have:

$$\left. \begin{array}{l}
\sum_{i=1}^4 \beta_i = 0 \\
\sum_{i=1}^4 \beta_i \dot{\rho}_i = 1
\end{array} \right\} \tag{11}$$

and

$$\sum_{i=1}^4 \frac{1}{\delta_i} \beta_i^2 = \min$$

where

$$\delta_2 = \delta_3 = 1$$

$$\delta_1 = \frac{T_2}{2T_1 + T_2} C \quad (C \text{ is a constant to be selected})$$

$$\delta_4 = \frac{T_2}{2T_3 + T_2} C$$

$$T_i = \dot{\rho}_{i+1} - \dot{\rho}_i \quad (i=1, 2, 3)$$

By solving equations (11), we get

$$\beta_i = \delta_i \lambda \tau_i \quad (i=1, 2, 3, 4)$$

where

$$\lambda = 1 / \sum_{i=1}^4 \delta_i \tau_i^2$$

$$\tau_i = \dot{\rho}_i - \dot{\rho}_0$$

$$\dot{\rho}_0 = \sum_{i=1}^4 \delta_i \dot{\rho}_i / \sum_{i=1}^4 \delta_i$$

$$C = \max \left[ \frac{T_2 + T_3}{T_1 + T_2 + T_3}, \frac{T_1 + T_2}{T_1 + T_2 + T_3} \right]$$

Thus, the residuals of  $k$ -subgroup are

$$r_{kl} = y_{kl} - b_k \dot{\rho}_{kl} \quad (l=1, 2, 3, 4)$$

c) For each subgroup, the largest and smallest values of  $r_{kl}$  are rejected. And we can get the initial values  $a_{k0}$ ,  $b_{k0}$  from remained two data points through follows:

$$y_{kl} = a_{k0} + b_{k0} \dot{\rho}_{kl} \quad (j=1, 2)$$

d) Then calculation the object function of M-estimate used all observations for every subgroups:

$$U_k = \sum_{i=1}^N F\{y_i - a_{k0} - b_{k0} \dot{\rho}_i\} \quad (k=1, 2, \dots, n)$$

where  $F\{\cdot\}$  can be taken from (3), and the initial value of  $\sigma$  can be arbitrarily given, for example 0.5 meters.

e) Select the minimum value from  $U_k$  ( $k=1, 2, \dots, n$ ). Suppose  $k=m$ , that is

$$U_m = \min.$$

Then  $a_{m0}$  and  $b_{m0}$ , those are taken from  $m$ -subgroup, can be used as the initial values  $a_0, b_0$ . It is sure that the  $a_0$  and  $b_0$  are taken from 'good' observation points.

f) Then we can get

$$r_i = y_i - a_0 - b_0 \dot{\rho}_i \quad (i=1, 2, \dots, N)$$

$$\sigma_0^2 = \frac{1}{N-2} \sum_{i=1}^N r_i^2$$

Because  $a_0, b_0$  are obtained by two data points, they have just lower accuracy. From (5) to (8) and iterated until convergence, the accurate results  $a, b$  can be get as above.

g) After correcting range bias and time bias, we can get a polynomial in time as following:

$$\begin{aligned} \Delta \rho'_i &= y_i - a - b \dot{\rho}_i \\ &= a_0 + a_1 t_i + a_2 t_i^2 + a_3 t_i^3 + \dots \end{aligned}$$

Using M-estimator, the parameters of polynomial  $a_0, a_1, a_2, a_3, \dots$  can be solved.

## CONCLUSION AND DISCUSSION

Comparing with the LS estimator, M-estimator has its advantage as follows:



a) It can be preprocess observation data that contain a large amount of noises, for example , a pass for LAGEOS in daytime are shown in fig 1, (12/20/1991 8:45 UT). In this pass rate of noise is up to 70%.

b) At same accuracy, the order of polynomial fitting is only 4 using M-estimator, while the order is up to 6-8 or more with LS estimator. Seeing table 1.

c) Noise mixed at the parts near the both ends of the curve can be detected and deleted.

Besides, comparison with the method of screen-processin and LS estimator, one third time is saved with M-estimator.

#### REFERENCE

J. peizhang                      On Joint Robust Estimation of The  
Parameters and The Variance.                      Acta Astronomica  
Sinica. Vol. 33. No 1. 1992.

Table 1.  
Comparison for Two Estimators(Lageos)

Passes Y M D H	M-estimator			LS-estimator		
	Order	RMS(cm)	Points	Order	RMS(cm)	Points
92011011	4	5.8	28	8	5.9	29
92011110	4	5.9	778	8	5.7	752
92011120	4	5.1	452	8	5.4	419
92011317	4	6.0	216	4	6.6	212
92011321	4	4.8	170	4	5.0	169
92011416	4	4.6	169	8	5.1	169
92011419	4	5.9	94	8	5.9	86
92011512	4	5.4	457	8	5.8	453
92022216	4	6.2	187	8	6.1	183
92031116	4	5.6	326	8	6.1	326
92041514	4	5.3	425	8	5.9	422
92041616	4	4.9	419	8	7.0	417
92042011	6	5.6	60	8	5.3	56
92042018	4	5.3	41	4	5.8	41
92042613	4	5.1	583	4	6.4	585
92043015	4	4.1	77	8	5.3	83
92050815	4	3.1	91	8	2.9	91
92052114	4	2.7	212	16	2.7	210
92052312	4	2.6	170	12	2.5	170
92060216	4	3.2	503	8	2.9	471

Fig. 1.  
Residual for A Lageos Pass in Daytime

